Optimal Energy-Efficient Relay Deployment for the Bidirectional Relay Transmission Schemes

Qimei Cui, *Member, IEEE*, Xianjun Yang, Jyri Hämäläinen, *Member, IEEE*, Xiaofeng Tao, *Senior Member, IEEE*, and Ping Zhang, *Member, IEEE*

***Abstract*—Recently, the energy efficiency of a relay network has become a hot research topic in the wireless communication society. In this paper, we investigate the energy efficiency of three basic bidirectional relay transmission schemes [i.e., the four time-slot (4TS), three time-slot (3TS), and two time-slot (2TS) schemes] from the angle of relay deployment. Since a realistic power consumption model is very important in analyzing energy efficiency, and a power amplifier (PA) consumes up to 70% of the total power, we consider a realistic nonideal PA model. The derived closed-form expressions for the optimal relay deployment and the simulation results reveal the following important conclusions. First, it is possible to achieve the optimal energy efficiency and enlarge the cell coverage simultaneously in bad channel conditions, but it may be very challenging in good channel conditions. Second, under asymmetric traffic conditions, particularly when the downlink rate is larger than the uplink rate, all the aforementioned three schemes have almost the same optimal relay deployment, but the 2TS scheme has the highest energy efficiency when the spectral efficiency is large. Third, the relay node should be deployed closer to the base station with the nonideal PA than that with the ideal PA, and the optimal energy efficiency with the nonideal PA is much higher than that with the ideal PA. Moreover, the impact of small-scale fading depends on the value of path loss. To overcome the small-scale fading, the relay network needs to consume more energy.**

***Index Terms*—Bidirectional relay transmissions, energy efficiency, network coding, non-ideal power amplifier, relay deployment.**

Manuscript received September 1, 2012; revised July 23, 2013 and October 16, 2013; accepted December 3, 2013. Date of publication December 19, 2013; date of current version July 10, 2014. This work was supported in part by the Beijing Nova Program under Grant xx2012037, by the Program for New Century Excellent Talents in University under Grant NCET12-0795, by the Beijing Higher Education Young Elite Teacher Project under Grant YETP0429, by the Key National Science Foundation of China under Grant 61231009, and by the National Science and Technology Major Project of China under Grant 2012ZX03001039-002. The review of this paper was coordinated by Prof. C. Assi.

Q. Cui, X. Tao, and P. Zhang are with the Key Laboratory of Universal Wireless Communications, Ministry of Education, Beijing University of Posts and Telecommunications, Beijing 100044, China (e-mail: cuiqimei@bupt.edu.cn; taoxf@bupt.edu.cn; pzhang@bupt.edu.cn).

X. Yang is with the Key Laboratory of Universal Wireless Communications, Ministry of Education, Beijing University of Posts and Telecommunications, Beijing 100044, China, and also with Macquarie University, Sydney, N.S.W. 2109, Australia (e-mail: yangxianjun67@gmail.com).

J. Hämäläinen is with the Department of Communications and Networking, Aalto University, 00076 Aalto, Finland (e-mail: jyri.hamalainen@aalto.fi).

Color versions of one or more of the figures in this paper are available online at http://ieeexplore.ieee.org.

Digital Object Identifier 10.1109/TVT.2013.2295413

I. Introduction

ALTHOUGH relay technology was first proposed to extend the cell coverage and improve the capacity of wireless communication networks [1], now, it is also recognized as an effective approach to reducing the energy consumption of wireless communication networks [2], [3]. The traditional relay technology needs four time slots (4TS) to complete the bidirectional communication. However, with the help of network coding (NC) [4] and physical NC (PNC) [5] techniques, relay technology can complete the bidirectional communication in three time slots (3TS) [6] and two time slots (2TS) [7], respectively. In this paper, we will investigate the energy efficiency of the aforementioned three relay transmission schemes via minimizing the sum of the energy consumption of the base station (BS), the relay node (RN), and the user equipment (UE) under certain transmission rate constraints.

A. Related Work

Current research on the energy efficiency of relay technology can be classified into the following two categories.

The first category focuses on investigating whether relay is always more energy efficient than direct transmission and which relay transmission scheme is the most energy efficient under certain conditions. Specifically, Zhang *et al.* [8] proved that, when considering the realistic nonlinear battery model, relay technology does not always increase the system energy efficiency. He and Li in [9] indicated that the two-hop relay scheme is more energy efficient than the direct transmission scheme when the channel condition is poor and gradually becomes worse under good channel conditions. In [10], Yao *et al.* found that the relay transmission with the decode-and-forward (DF) protocol has higher energy efficiency than that with the amplify-and-forward (AF) protocol when the distance between the source node and the RN is not very large. Sun and Yang [11] found that the 2TS scheme has higher energy efficiency than that of direct transmission and the 4TS scheme in symmetric systems, where the circuit power consumption at each node is identical, and the downlink transmission rate is equal to the uplink transmission rate.

The second category mainly focuses on studying how to achieve the highest energy efficiency for certain relay transmission schemes. Generally speaking, the energy efficiency of the relay system can be maximized via resource allocation [12]–[15], relay deployment [16]–[18], or joint resource allocation and relay deployment/selection [19]–[21]. Specifically, two

dynamic subband allocation schemes were proposed in [12] to improve the energy efficiency of DF-based opportunistic relay in a single-carrier frequency-division multiple-access system. Abuzainab and Ephremides in [13] proposed an optimal power-allocation scheme to minimize the energy consumed in the cooperative relay network. Then, an energy-efficient power-allocation scheme was proposed in [14] for fixed-gain AF relay networks with partial channel state information. Recently, an energy-optimal and rate-optimal power-allocation scheme has been proposed in [15] for a DF-based relay channel.

Regarding relay deployment, Li *et al.* in [16] indicated that, to minimize the energy consumption of the 2TS relay transmission scheme, the RN is best positioned at the middle point of the two end nodes for any asymmetric traffic requirements. Khirallah *et al.* in [17] investigated the impacts of energy and cost on relay deployment in the heterogeneous long-term evolution advanced (LTE-A) network. Then, Wu and Feng in [18] found that, by introducing an appropriate number of RNs with proper locations into cellular networks, energy efficiency can be improved without compromising system throughput. Furthermore, Lin and Lin in [19] proposed a joint relay-placement and bandwidth-allocation scheme to minimize the total cost of RNs as well as to meet the minimal traffic demand for each UE. Zhou *et al.* in [20] proposed an optimal energy-efficient relay-selection and power-allocation scheme for 2TS relay transmission, whereas Ho and Huang in [21] proposed an energy-efficient subcarrier-power-allocation and relay-selection scheme for cooperative relay networks.

It is worthwhile to note that the power consumption model plays a very important role in the given research on the energy efficiency of a relay system. Since the power amplifiers (PAs) consume up to 70% of the total power [22], the PA model is the most important part of the power consumption model. All of the aforementioned literatures only consider the ideal PA model, where the PA efficiency remains constant for varying values of the PA output power. However, in reality, the PAs are always nonideal, where the PA efficiency changes with the PA output power. This change causes an important problem that needs to be further investigated: What is the impact of the nonideal PA on the energy efficiency of relay systems in comparison with that of the ideal PA?

B. Our Contributions

Since relay deployment is the first step to establishing a relay network and is a critical task in network planning to achieve an efficient and scalable network environment, we mainly focus on the research of energy-efficient relay deployment for the 4TS, 3TS, and 2TS schemes with the nonideal PA.

The optimal energy-efficient relay deployment is achieved by solving optimization problems of minimizing the energy consumption index (ECI) under the bidirectional sum rate constraint. However, with the nonideal PA, the objective function of the given optimization problem with the nonideal PA becomes more complicated than that with the ideal PA. Specifically, the objective function of the optimization problem becomes a sum of three variants, which are the square roots of the inverse-logarithmic function of the PA output power for the BS, the RN, and the UE, respectively.

After deriving the closed-form expressions from these optimization problems, the correctness of the theoretical derivation is validated by numerical simulation results. Then, the energy efficiencies for 4TS, 3TS, and 2TS schemes are compared against each other at their optimal relay deployments. Afterward, we investigate the impact of the nonideal PA on the optimal relay deployment and the relative ECI in comparison with that of the ideal PA model via theoretical analysis and simulation results. Finally, we study the derived optimal relay deployments under more practical situations, e.g., the long-term evolution (LTE) outdoor rural scenario and the scenario with small-scale fading.

Via theoretical analysis and numerical simulation results, we obtain the following important conclusions. First, it is possible to achieve the optimal energy efficiency and extend the cell coverage simultaneously in bad channel conditions, e.g., heavy path loss. However, it is very challenging to realize the aforementioned two goals at the same time in good channel conditions, e.g., small path loss. Second, under an asymmetric traffic condition, when the downlink rate is larger than the uplink rate, the 4TS, 3TS, and 2TS schemes have almost the same optimal relay deployment. However, when the downlink rate is smaller than the uplink rate, the optimal relay deployments for these three schemes have very different trends. Third, when the spectral efficiency is high, the 2TS scheme is the most energy efficient at the optimal relay deployment, in comparison with the 3TS and 4TS schemes. On the contrary, when the spectral efficiency is low, the 4TS scheme is the most energy efficient at the optimal relay deployment among these three schemes.

Furthermore, the impact of the nonideal PA on the optimal relay deployment is that it requires the RN to be deployed nearer to the BS than that with the ideal PA. The energy efficiency at the optimal relay deployment with the nonideal PA is higher than that with the ideal PA. Finally, the impact of small-scale fading depends on the value of path loss. Specifically, when the path loss is very small, the RN should be deployed farther from the BS than that without small-scale fading. On the contrary, when the path loss is large, the RN should be deployed nearer to the BS than that without small-scale fading. In addition, compared with the scenario without small-scale fading, the transmission nodes need to consume more energy to overcome small-scale fading.

The rest of this paper is organized as follows: In Section II, we introduce the channel model and the power consumption model and then formulate the optimization problem. In Section III, we present the closed-form expressions for the optimal energy-efficient deployments and the relative ECI for these three basic bidirectional relay transmission schemes. In Section IV, we first validate the correctness of the theoretical derivations through numerical simulation results, and we then investigate the impacts of spectral efficiency, channel conditions, and the ratio of the downlink rate to the sum of the uplink rate and the downlink rate on the optimal relay deployment and the relative ECI. Finally, this paper is concluded in Section V.

Moreover, the meanings of the main symbols in this paper are listed in Table I to make them clearer and easier to read.

TABLE I
LIST OF THE SYMBOL MEANINGS

Symbols	Meanings
α	Path loss exponent.
β	Ratio of downlink rate $R_{BS\to UE}$ to sum rate R_s.
η_{se}	Spectral efficiency.
μ_1, μ_2	$\mu_1 = 2^{4\beta\eta_{se}}$ and $\mu_2 = 2^{4(1-\beta)\eta_{se}}$.
μ_3, μ_4	$\mu_3 = 2^{3\beta\eta_{se}}$ and $\mu_4 = 2^{3(1-\beta)\eta_{se}}$.
μ_5, μ_6	$\mu_5 = 2^{2\beta\eta_{se}}$ and $\mu_6 = 2^{2(1-\beta)\eta_{se}}$.
η_{ECI}	Energy Consumption Index (ECI).
$\eta_{PA,i}$	PA efficiency of node i (e.g., BS, RN or UE).
ρ_i	$\sqrt{p_{max,i}}/\eta_{PA,i}$, where $p_{max,i}$ is the maximum designed output power of PA in node i.
$\theta_{DC,i}$	Loss factor of the DC-DC power supply in node i.
$\theta_{MS,i}$	Loss factor of the Main Supply in node i.
$\theta_{cool,i}$	Loss factor of the cooling in node i.
γ_i	$1/[(1-\theta_{DC,i})(1-\theta_{MS,i})(1-\theta_{cool,i})]$.
τ_0	An unitless constant which depends on the antenna characteristics and the average channel attenuation.
d_0	The reference distance for the antenna far-field.
$d_{i\to j}$	The distance between node i and node j.
g	$d_{BS\to RN}/d_{RN\to UE}$.
p	Power consumption.
f_c	Carrier frequency.
A_{ij}, B_{ij}	Coefficients in the expressions for the optimal relay deployment.
B	Signal bandwidth.
D	Distance between BS and UE.
$P_{out,i}$	The transmit power of PA in node i.
$P_{tot,i}$	The total power consumption of node i.
$P_{RF,i}$	The power consumption of the RF part in node i.
$P_{C,i}$	The constant power consumed by the other parts of node i.
C_{kTS}	The sum of $P_{RF,i}$ of BS, relay and UE in the kTS scheme, where k = 2, 3 or 4.
P_s	The sum of the total power consumption of BS, relay and UE.
$R_{i\to j}$	The transmission rate from node i to node j.
R_s	The sum of downlink rate and uplink rate.

II. SYSTEM MODEL AND PROBLEM FORMULATION

In this paper, we consider a wireless bidirectional relay network where the BS and the UE communicate with each other through an RN. Here, we assume that the DF protocol is used in the relay network, since DF can achieve the ergodic capacity when the RN is near the source node [23].

A. Three Basic Bidirectional Relay Transmission Schemes

In this paper, we consider the following three transmission schemes, which differ in the number of time slots required to finish the bidirectional relay communication process.

1) 4TS Transmission: As shown in Fig. 1(a), the BS and the UE need 4TS to complete the bidirectional communication in this traditional scheme. In the first time slot, the BS transmits its signal to an RN. In the second time slot, the RN decodes and forwards the received signal to the UE. In the third time slot, the UE transmits its signal to the RN. In the fourth time slot, the RN decodes and forwards the received signal to the BS.

2) 3TS Transmission: Fig. 1(b) demonstrates how the BS and the UE communicate with each other using the NC [4] technique over 3TS with the help of an RN. In the first time slot, the BS transmits its signal to an RN, and then, the RN decodes the received signal. In the second time slot, the UE transmits its signal to the RN, and then, the RN decodes the received data. In the third time slot, the RN broadcasts a linear combination of the decoded data to the BS and the UE.

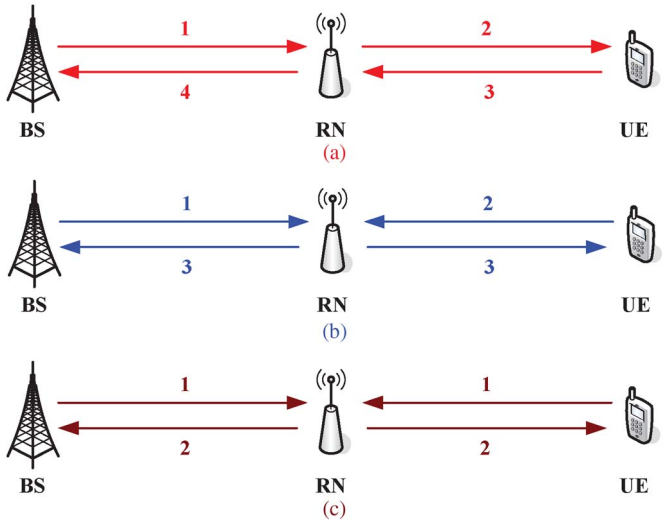

Fig. 1. Three basic bidirectional relay transmission schemes. (a) 4TS transmission scheme. (b) 3TS transmission scheme. (c) 2TS transmission scheme.

3) 2TS Transmission: Fig. 1(c) shows that the bidirectional relay transmission can be completed in 2TS if the PNC [5] technique is used. In the first time slot, the BS and the UE simultaneously transmit their own signals to an RN using the nested lattice codes [7]. In the second time slot, the RN broadcasts a structured binning of signals to the BS and the UE, and then, the BS and the UE decode the received signal by exploiting this binning information together with their own signals [7].

B. Channel Model

We assume that the value of the noise power at each node is the same, i.e., $\sigma^2_{\rm BS} = \sigma^2_{\rm UE} = \sigma^2_{\rm RN} = \sigma^2 = N_0 B$, where N_0 is the power spectral density, and B is the signal bandwidth. To simplify the derivation, we consider the additive white Gaussian noise channel with the large-scale path loss [24]. Thus, the received power at node j (e.g., BS, RN, or UE) from node i is

$$P_{{\rm rec},i\to j} = \tau_0 \left(\frac{d_0}{d_{i\to j}}\right)^{\alpha} P_{{\rm out},i} \tag{1}$$

where $P_{{\rm out},i}$ is the transmit power of node i, α is the path loss exponent, τ_0 is a unitless constant that depends on the antenna characteristics and the average channel attenuation, d_0 is the reference distance for the antenna far-field, and $d_{i\to j}$ is the distance between node i and node j. If we let $h_{i\to j}$ be the channel coefficient from node i to node j, then we have

$$|h_{i\to j}|^2 = \tau_0 \left(\frac{d_0}{d_{i\to j}}\right)^{\alpha}. \tag{2}$$

As shown in Fig. 2, in this paper, we assume that the RN is deployed along the line between the BS and the UE and denote

$$g = \frac{d_{\rm RN\to UE}}{d_{\rm BS\to RN}}. \tag{3}$$

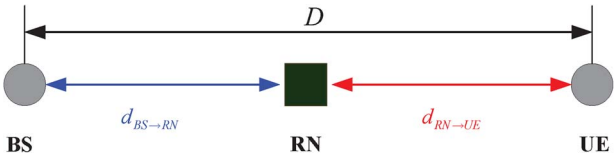

Fig. 2. Relay deployment.

If we let D denote the distance between the BS and the UE, then we have

$$d_{\mathrm{BS}\to\mathrm{RN}} = \frac{1}{1+g}D, \qquad d_{\mathrm{RN}\to\mathrm{UE}} = \frac{g}{1+g}D \tag{4}$$

which will be used to formulate the results in Section III.

C. Power Consumption Model

According to the power consumption model for LTE BS in Energy Aware Radio and neTwork tecHnologies (EARTH) project [25], the total power consumption of the BS at the maximum load is expressed as

$$P_{\mathrm{tot,BS}} = \frac{p_{\mathrm{PA,BS}} + p_{\mathrm{BB}} + p_{\mathrm{ss}}}{(1-\theta_{\mathrm{dc}})(1-\theta_{\mathrm{MS}})(1-\theta_{\mathrm{cool}})} \tag{5}$$

where $p_{\mathrm{PA,BS}}$ is the energy consumption of the PA in the BS, p_{BB} is the energy consumption of baseband (BB) digital signal processing, p_{ss} is the energy consumption of the small-signal transceiver, and θ_{dc}, θ_{MS}, and θ_{cool} are the loss factors of direct-current-to-direct-current (dc–dc) power supply, main supply, and cooling, respectively. The power consumption of the RN can be approximated by that of pico evolved Node B (eNB) [26], i.e., the energy consumption of the RN can be modeled by (5) with the parameters for Pico eNB in [25].

In reality, the UE is usually in idle state with certain probability, and the energy consumption model for LTE UE [27] is

$$\begin{aligned} P_{\mathrm{tot,UE}} = {} & m_{\mathrm{idle}}p_{\mathrm{idle}} \\ & + \overline{m_{\mathrm{idle}}}\Big\{p_{\mathrm{con}} + m_{\mathrm{Tx}}m_{\mathrm{Rx}}p_{\mathrm{Tx+Rx}} \\ & \quad + m_{\mathrm{Tx}}[p_{\mathrm{Tx}} + p_{\mathrm{PA,Tx}} + p_{\mathrm{RxBB}}] \\ & \quad + m_{\mathrm{Rx}}[p_{\mathrm{Rx}} + p_{\mathrm{PA,Rx}} + p_{\mathrm{RxBB}}]\Big\} \end{aligned} \tag{6}$$

where the logical variable m_{state} represents the mode, which can be radio resource configuration (RRC) idle or RRC connected (con), transmitting (Tx) and receiving (Rx), with $\overline{m_{\mathrm{idle}}} = 1 - m_{\mathrm{idle}}$ denotes the nonidle state. p is the power consumption, where subscripts $_{\mathrm{idle}}$ and $_{\mathrm{con}}$ represent the power consumption in RRC idle and connected mode, respectively; subscripts $_{\mathrm{PA,Tx}}$ and $_{\mathrm{PA,Rx}}$ denote the power consumption of the PA in the Rx and Tx chains, respectively; subscripts $_{\mathrm{TxBB}}$ and $_{\mathrm{RxBB}}$ represent the power consumption of the baseband parts in the Rx and Tx chains, respectively; and subscripts $_{\mathrm{Tx}}$, $_{\mathrm{Rx}}$, and $_{\mathrm{Tx+Rx}}$ denote the power consumed when the Rx chain, the Tx chain, and both the Rx and Tx chains are active, respectively.

To facilitate the derivations of the optimal energy-efficient relay deployments, the given power consumption models for the BS, the RN, and the UE are generalized as

$$P_{\mathrm{tot},i} = P_{\mathrm{RF},i} + P_{C,i} \tag{7}$$

where $P_{\mathrm{RF},i}$ is the power consumption of the RF part in node i (e.g., BS, RN, or UE), and $P_{C,i}$ is the constant power consumed by the other parts of node i. Specifically, for the BS and the RN, we have $P_{\mathrm{RF},i} = \gamma_i p_{\mathrm{PA},i}$ and $P_{C,i} = \gamma_i(p_{\mathrm{BB}} + p_{\mathrm{ss}})$, where $\gamma_i = 1/[(1-\theta_{\mathrm{dc},i})(1-\theta_{\mathrm{MS},i})(1-\theta_{\mathrm{cool},i})]$. For the UE, we have $P_{\mathrm{RF,UE}} = \overline{m_{\mathrm{idle}}}\{m_{\mathrm{Tx}}p_{\mathrm{TxPA}} + m_{\mathrm{Rx}}p_{\mathrm{RxPA}}\}$ and $P_{C,\mathrm{UE}} = P_{\mathrm{tot,UE}} - P_{\mathrm{PA,UE}}$. Assuming that $p_{\mathrm{PA,Tx}} = p_{\mathrm{PA,Rx}} = p_{\mathrm{PA,UE}}$, we have $P_{\mathrm{RF,UE}} = \overline{m_{\mathrm{idle}}}p_{\mathrm{PA,UE}}$.

In contrast with the constant PA efficiency for the ideal PA, the efficiency of the nonideal PA varies with the change in the output power. With the nonconstant envelope signals, the orthogonal frequency-division multiplexing modulation in an LTE system requires the PA to operate in a more linear region. Thus, this paper considers the following nonideal linear PA, whose power consumption for node i is approximated as [30]

$$p_{\mathrm{PA},i} = \frac{\sqrt{p_{\mathrm{max},i}}}{\eta_{\mathrm{PA},i}^{\max}}\sqrt{P_{\mathrm{out},i}} \triangleq \rho_i\sqrt{P_{\mathrm{out},i}}. \tag{8}$$

Thus, the PA efficiency of node i is expressed as

$$\eta_{\mathrm{PA},i} = \frac{P_{\mathrm{out},i}}{p_{\mathrm{PA},i}} = \sqrt{\frac{P_{\mathrm{out},i}}{p_{\mathrm{max},i}}}\eta_{\mathrm{PA},i}^{\max} \tag{9}$$

where $p_{\mathrm{max},i}$ is the maximum designed output power of the PA in node i, $\eta_{\mathrm{PA},i}^{\max}$ is the PA efficiency of node i at maximum designed power, and ρ_i is a constant and defined as $\sqrt{p_{\mathrm{max},i}}/\eta_{\mathrm{PA},i}^{\max}$. Expression (9) shows that the value of $\eta_{\mathrm{PA},i}$ changes with the transmitter output power $P_{\mathrm{out},i}$.

D. Problem Formulation

We investigate the optimal energy-efficient relay deployment under the constraint of fixed bidirectional sum rate R_s. To measure the energy efficiency of the relay network, we adopt the following defined ECI:

$$\eta_{\mathrm{ECI}} = P_s/R_s \tag{10}$$

where P_s is the sum of the total power consumption of the BS, the RN, and the UE, and R_s is the sum of the downlink rate and the uplink rate. The optimization problem is formulated as

$$\begin{aligned} \min_{g} \quad & \eta_{\mathrm{ECI}}(g) = \frac{P_s}{R_s} \\ \text{s.t.} \quad & R_{\mathrm{BS}\to\mathrm{UE}} = \beta R_s \\ & R_{\mathrm{UE}\to\mathrm{BS}} = (1-\beta)R_s \end{aligned} \tag{11}$$

where $R_{\mathrm{BS}\to\mathrm{UE}}$ is the downlink rate from the BS to the UE, $R_{\mathrm{UE}\to\mathrm{BS}}$ is the uplink rate from the UE to the BS, and β is the ratio of $R_{\mathrm{BS}\to\mathrm{UE}}$ to R_s with $0 < \beta < 1$. The relationship

between the optimization objective function $\eta_{\mathrm{ECI}}(g)$ and the optimization variable g will be elaborated in the Appendix.

III. Optimal Relay Deployment for These Three Transmission Schemes

Here, we present the closed-form expressions for the optimal relay deployment and the corresponding ECI for 4TS, 3TS, and 2TS transmission schemes with the DF protocol.

A. Optimal Relay Deployment and the Corresponding ECI for 4TS Transmission Scheme

Theorem 1: If the DF protocol is used in the 4TS bidirectional relay transmission, then the optimal energy-efficient relay deployment is

$$d_{\mathrm{RN}\to\mathrm{UE}}^{4\mathrm{TS}} = g_{4\mathrm{TS,opt}} d_{\mathrm{BS}\to\mathrm{RN}}^{4\mathrm{TS}} \tag{12}$$

with

$$g_{4\mathrm{TS,opt}} = \left(\frac{\rho_{\mathrm{BS}}\gamma_{\mathrm{BS}}\sqrt{\mu_1 - 1} + \rho_{\mathrm{RN}}\gamma_{\mathrm{RN}}\sqrt{\mu_2 - 1}}{\rho_{\mathrm{UE}}\overline{m_{\mathrm{idle}}}\sqrt{\mu_2 - 1} + \rho_{\mathrm{RN}}\gamma_{\mathrm{RN}}\sqrt{\mu_1 - 1}} \right)^{\frac{2}{\alpha-2}} \tag{13}$$

where $\mu_1 = 2^{4\beta\eta_{\mathrm{se}}}$, $\mu_2 = 2^{4(1-\beta)\eta_{\mathrm{se}}}$, and $\eta_{\mathrm{se}} = R_s/B$ are the spectral efficiency.

In addition, the ECI of the 4TS scheme at the optimal relay deployment is

$$\eta_{\mathrm{ECI,4TS}}^{\mathrm{opt}} = A_{1,2}\left(\frac{1}{1+g_{4\mathrm{TS,opt}}}\right)^{\frac{\alpha}{2}} + B_{1,2}\left(\frac{g_{4\mathrm{TS,opt}}}{1+g_{4\mathrm{TS,opt}}}\right)^{\frac{\alpha}{2}} + \frac{C_{4\mathrm{TS}}}{R_s} \tag{14}$$

where the expressions for $A_{1,2}$ and $B_{1,2}$ are

$$\begin{aligned} A_{1,2} &= E_1\left(\rho_{\mathrm{BS}}\gamma_{\mathrm{BS}}\sqrt{\mu_1 - 1} + \rho_{\mathrm{RN}}\gamma_{\mathrm{RN}}\sqrt{\mu_2 - 1}\right) \\ B_{1,2} &= E_1\left(\rho_{\mathrm{UE}}\overline{m_{\mathrm{idle}}}\sqrt{\mu_2 - 1} + \rho_{\mathrm{RN}}\gamma_{\mathrm{RN}}\sqrt{\mu_1 - 1}\right) \end{aligned} \tag{15}$$

where $E_1 = (\sigma D^{\alpha/2})/(4R_s d_0^{\alpha/2}\sqrt{\tau_0})$, and $C_{4\mathrm{TS}} = (P_{C,\mathrm{BS}} + P_{C,\mathrm{UE}} + 2P_{C,\mathrm{RN}})/4$ is the sum of the constant power consumed by other parts beside the RF part in the BS, the RN, and the UE in the 4TS transmission scheme.

Proof: See Appendix A. ■

Remark: Since $d_{\mathrm{BS}\to\mathrm{RN}}/D = 1/(1+g_{\mathrm{opt}})$, we adopt $1/(1+g_{\mathrm{opt}})$ to denote the optimal relay deployment. First, we can infer that the base of the exponentiation in (13) is greater than 1, because of the relationship $\rho_{\mathrm{BS}} > \rho_{\mathrm{RN}} > \rho_{\mathrm{UE}}$, which is due to $p_{\max,\mathrm{BS}} > p_{\max,\mathrm{RN}} > p_{\max,\mathrm{UE}}$ in (8). Thus, we can obtain the conclusion that the optimal relay deployment $1/(1+g_{4\mathrm{TS,opt}})$ is a monotonically increasing function of α. However, the relationships between $1/(1+g_{4\mathrm{TS,opt}})$ and β, η_{se} are not monotonous, and we will investigate these relationships via numerical simulations in Section IV. According to (14) and (15), we can infer that the ECI at the optimal relay deployment $\eta_{\mathrm{ECI,4TS}}^{\mathrm{opt}}$ monotonously increases with the increase of α and η_{se}, whereas the relationship between $\eta_{\mathrm{ECI,4TS}}^{\mathrm{opt}}$ and β is not monotonous.

B. Optimal Relay Deployment and the Corresponding ECI for 3TS Transmission Scheme

Theorem 2: If the DF protocol is used in the 3TS bidirectional relay transmission, then the optimal energy-efficient relay deployment is

$$d_{\mathrm{RN}\to\mathrm{UE}}^{3\mathrm{TS}} = g_{3\mathrm{TS,opt}} d_{\mathrm{BS}\to\mathrm{RN}}^{3\mathrm{TS}} \tag{16}$$

with

$$g_{3\mathrm{TS,opt}} = \begin{cases} g_2, & \text{if } g_2 < g_{3\mathrm{TS,th}} \\ g_1, & \text{if } g_1 \geq g_{3\mathrm{TS,th}} \\ g_{3\mathrm{TS,th}}, & \text{otherwise} \end{cases} \tag{17}$$

where

$$\begin{aligned} g_2 &= \left(\frac{\rho_{\mathrm{BS}}\gamma_{\mathrm{BS}}\sqrt{\mu_3 - 1} + \rho_{\mathrm{RN}}\gamma_{\mathrm{RN}}\sqrt{\mu_4 - 1}}{\rho_{\mathrm{UE}}\overline{m_{\mathrm{idle}}}\sqrt{\mu_4 - 1}}\right)^{\frac{2}{\alpha-2}} \\ g_1 &= \left(\frac{\rho_{\mathrm{BS}}\gamma_{\mathrm{BS}}\sqrt{\mu_3 - 1}}{\rho_{\mathrm{UE}}\overline{m_{\mathrm{idle}}}\sqrt{\mu_4 - 1} + \rho_{\mathrm{RN}}\gamma_{\mathrm{RN}}\sqrt{\mu_3 - 1}}\right)^{\frac{2}{\alpha-2}} \\ g_{3\mathrm{TS,th}} &= \left(\frac{\sqrt{\mu_4 - 1}}{\sqrt{\mu_3 - 1}}\right)^{\frac{2}{\alpha}} \end{aligned} \tag{18}$$

where $\mu_3 = 2^{3\beta\eta_{\mathrm{se}}}$, and $\mu_4 = 2^{3(1-\beta)\eta_{\mathrm{se}}}$.

In addition, the ECI of the 3TS scheme at the optimal relay deployment is

$$\eta_{\mathrm{ECI,3TS}}^{\mathrm{opt}} = \begin{cases} f_{3\mathrm{TS},2}(g_2), & \text{if } g_2 < g_{3\mathrm{TS,th}} \\ f_{3\mathrm{TS},1}(g_1), & \text{if } g_1 \geq g_{3\mathrm{TS,th}} \\ f_{3\mathrm{TS},1}(g_{3\mathrm{TS,th}}), & \text{otherwise} \end{cases} \tag{19}$$

where the expressions for $f_{3\mathrm{TS},1}(g)$ and $f_{3\mathrm{TS},2}(g)$ are

$$\begin{aligned} f_{3\mathrm{TS},1}(g) &= A_{2,2}\left(\frac{1}{1+g}\right)^{\frac{\alpha}{2}} + B_{2,2}\left(\frac{g}{1+g}\right)^{\frac{\alpha}{2}} + \frac{C_{3\mathrm{TS}}}{R_s} \\ f_{3\mathrm{TS},2}(g) &= A_{2,3}\left(\frac{1}{1+g}\right)^{\frac{\alpha}{2}} + B_{2,3}\left(\frac{g}{1+g}\right)^{\frac{\alpha}{2}} + \frac{C_{3\mathrm{TS}}}{R_s} \end{aligned} \tag{20}$$

where $C_{3\mathrm{TS}} = (P_{C,\mathrm{BS}} + P_{C,\mathrm{UE}} + P_{C,\mathrm{RN}})/3$ is the sum of the constant power consumed by other parts beside the RF part in the BS, the relay, and the UE in the 3TS transmission scheme. The expressions for the coefficients $A_{2,2}$, $B_{2,2}$, $A_{2,3}$, and $B_{2,3}$ are

$$\begin{aligned} A_{2,2} &= E_2\left(\rho_{\mathrm{BS}}\gamma_{\mathrm{BS}}\sqrt{\mu_3 - 1}\right) \\ B_{2,2} &= E_2\left(\rho_{\mathrm{UE}}\overline{m_{\mathrm{idle}}}\sqrt{\mu_4 - 1} + \rho_{\mathrm{RN}}\gamma_{\mathrm{RN}}\sqrt{\mu_3 - 1}\right) \\ A_{2,3} &= E_2\left(\rho_{\mathrm{BS}}\gamma_{\mathrm{BS}}\sqrt{\mu_3 - 1} + \rho_{\mathrm{RN}}\gamma_{\mathrm{RN}}\sqrt{\mu_4 - 1}\right) \\ B_{2,3} &= E_2\left(\rho_{\mathrm{UE}}\overline{m_{\mathrm{idle}}}\sqrt{\mu_4 - 1}\right) \end{aligned} \tag{21}$$

where $E_2 = (\sigma D^{\alpha/2})/(3R_s d_0^{\alpha/2}\sqrt{\tau_0})$.

Proof: See Appendix B. ■

Remark: Obviously, both g_{opt} in (17) and the relative ECI in (19) are piecewise functions. Since both the bases of the exponentiations of g_1 and g_2 are greater than 1, then the optimal relay deployment $1/(1+g_{3\text{TS,opt}})$ is an increasing function of α if $g_2 < g_{3\text{TS,th}}$ and $g_1 \geq g_{3\text{TS,th}}$. The relationships between $1/(1+g_{3\text{TS,opt}})$ and β, η_{se} are not monotonous, and we will investigate these relationships via numerical simulations in Section IV. From the expressions in (19)–(21), we can see that $\eta_{\text{ECI,3TS}}^{\text{opt}}$ monotonously increases with the increase of α and η_{se}, whereas the relationship between $\eta_{\text{ECI,3TS}}^{\text{opt}}$ and β is not monotonous.

C. Optimal Relay Deployment and the Corresponding ECI for 2TS Transmission Scheme

Theorem 3: If the lattice encoding and decoding method [7] is used in the 2TS bidirectional relay transmission, then the optimal energy-efficient relay deployment is

$$d_{\text{RN}\to\text{UE}}^{\text{2TS}} = g_{\text{2TS,opt}} d_{\text{BS}\to\text{RN}}^{\text{2TS}} \tag{22}$$

with

$$g_{\text{2TS,opt}} = \begin{cases} g_4, & \text{if } g_4 < g_{\text{2TS,th}} \\ g_3, & \text{if } g_3 \geq g_{\text{2TS,th}} \\ g_{\text{2TS,th}}, & \text{otherwise} \end{cases} \tag{23}$$

where

$$\begin{aligned} g_4 &= \left(\frac{\rho_{\text{BS}}\gamma_{\text{BS}}\nu_1 + \rho_{\text{RN}}\gamma_{\text{RN}}\nu_3}{\rho_{\text{UE}}\overline{m_{\text{idle}}}\nu_4}\right)^{\frac{2}{\alpha-2}} \\ g_3 &= \left(\frac{\rho_{\text{BS}}\gamma_{\text{BS}}\nu_1}{\rho_{\text{UE}}\overline{m_{\text{idle}}}\nu_2 + \rho_{\text{RN}}\gamma_{\text{RN}}\nu_4}\right)^{\frac{2}{\alpha-2}} \\ g_{\text{2TS,th}} &= \left(\frac{\sqrt{\mu_6-1}}{\sqrt{\mu_5-1}}\right)^{\frac{2}{\alpha}} \end{aligned} \tag{24}$$

where

$$\begin{aligned} &\nu_1 = \sqrt{\mu_5(\mu_5+\mu_6-1)}, \quad \nu_2 = \sqrt{\mu_5(\mu_5+\mu_6-1)} \\ &\nu_3 = \sqrt{(\mu_5+\mu_6)(\mu_6-1)}, \quad \nu_4 = \sqrt{(\mu_5+\mu_6)(\mu_5-1)} \end{aligned} \tag{25}$$

where $\mu_5 = 2^{2\beta\eta_{\text{se}}}$, and $\mu_6 = 2^{2(1-\beta)\eta_{\text{se}}}$.

In addition, the ECI of the 2TS scheme at the optimal relay deployment is

$$\eta_{\text{ECI,2TS}}^{\text{opt}} = \begin{cases} f_{\text{2TS,2}}(g_4), & \text{if } g_4 < g_{\text{2TS,th}} \\ f_{\text{2TS,1}}(g_3), & \text{if } g_3 \geq g_{\text{2TS,th}} \\ f_{\text{2TS,1}}(g_{\text{2TS,th}}), & \text{otherwise} \end{cases} \tag{26}$$

where the expressions for $f_{\text{2TS,1}}(g)$ and $f_{\text{2TS,2}}(g)$ are

$$\begin{aligned} f_{\text{2TS,1}}(g) &= A_{3,3}\left(\frac{1}{1+g}\right)^{\frac{\alpha}{2}} + B_{3,3}\left(\frac{g}{1+g}\right)^{\frac{\alpha}{2}} + \frac{C_{\text{2TS}}}{R_s} \\ f_{\text{2TS,2}}(g) &= A_{3,4}\left(\frac{1}{1+g}\right)^{\frac{\alpha}{2}} + B_{3,4}\left(\frac{g}{1+g}\right)^{\frac{\alpha}{2}} + \frac{C_{\text{2TS}}}{R_s} \end{aligned} \tag{27}$$

where $C_{\text{2TS}} = (P_{C,\text{BS}} + P_{C,\text{UE}} + P_{C,\text{RN}})/2$ is the sum of the constant power consumed by other parts beside the RF part in the BS, the relay, and the UE in the 2TS transmission scheme. The expressions for the coefficients $A_{3,3}$, $B_{3,3}$, $A_{3,4}$, and $B_{3,4}$

$$\begin{aligned} A_{3,3} &= E_3\left(\rho_{\text{BS}}\gamma_{\text{BS}}\sqrt{\frac{\mu_5}{\mu_5+\mu_6}(\mu_5+\mu_6-1)}\right) \\ B_{3,3} &= E_3\left(\rho_{\text{UE}}\overline{m_{\text{idle}}}\sqrt{\frac{\mu_6}{\mu_5+\mu_6}(\mu_5+\mu_6-1)}\right. \\ &\qquad \left. + \rho_{\text{RN}}\gamma_{\text{RN}}\sqrt{\mu_5-1}\right) \\ A_{3,4} &= E_3\left(\rho_{\text{BS}}\gamma_{\text{BS}}\sqrt{\frac{\mu_5}{\mu_5+\mu_6}(\mu_5+\mu_6-1)}\right. \\ &\qquad \left. + \rho_{\text{RN}}\gamma_{\text{RN}}\sqrt{\mu_6-1}\right) \\ B_{3,4} &= E_3\left(\rho_{\text{UE}}\overline{m_{\text{idle}}}\sqrt{\frac{\mu_6}{\mu_5+\mu_6}(\mu_5+\mu_6-1)}\right) \end{aligned} \tag{28}$$

where $E_3 = (\sigma D^{\alpha/2})/(2R_s d_0^{\alpha/2}\sqrt{\tau_0})$.

Proof: See Appendix C. ■

Remark: Since the bases of the exponentiations of g_3 and g_4 are greater than 1, the optimal relay deployment $1/(1+g_{\text{2TS,opt}})$ is an increasing function of α if $g_4 < g_{\text{2TS,th}}$ and $g_3 \geq g_{\text{2TS,th}}$. The relationships between $1/(1+g_{\text{2TS,opt}})$ and β, η_{se} are not monotonous and will be investigated via numerical simulations in Section IV. From the expressions in (26)–(28), we can see that $\eta_{\text{ECI,2TS}}^{\text{opt}}$ monotonously increases with the increase of α and η_{se}, whereas the relationship between $\eta_{\text{ECI,2TS}}^{\text{opt}}$ and β is not monotonous.

IV. Performance Evaluation

In Section IV-A, the relative simulation parameters are stated. In Section IV-B, we verify the theoretical derivations and study the impacts of spectral efficiency, the path loss, and the ratio of the downlink rate to the sum of the uplink rate and the downlink rate on the optimal relay deployment and the relative ECI. In Section IV-C, we investigate the influence of the nonideal PA on the optimal relay deployment in comparison with that of the ideal PA via simulation results. Finally, in Section IV-D, we discuss the optimal relay deployment in more practical scenarios, such as the scenario with Rician small-scale fading and the scenario for the LTE system.

A. Simulation Parameters

Table II lists the power consumption parameters for the BS, the relay, and the UE, where the parameters for the BS and the relay are based on the EARTH project [25], and the parameters for the UE are based on [27]. In this paper, we assume that the UE is in idle state with probability 0.6, and the probability that the UE is in nonidle state is 0.45. The values of PA efficiencies for the BS, the relay, and the UE are based on [25], [28], and [29], respectively. The parameters used to verify theoretical derivations are listed in Table III, where the path loss constant

TABLE II
POWER CONSUMPTION PARAMETERS

Symbols	Values	Meanings
$\eta_{PA,BS}$	0.388 [25]	Power amplifier efficiency of BS
$\eta_{PA,RN}$	0.35 [28]	Power amplifier efficiency of RN
$\eta_{PA,UE}$	0.5 [29]	Power amplifier efficiency of UE
$p_{max,BS}$	53.3 dBm [30]	The maximum designed output power of the PA in BS
$p_{max,RN}$	35.9 dBm [30]	The maximum designed output power of the PA in RN
$p_{max,UE}$	26.7 dBm [30]	The maximum designed output power of the PA in UE
$p_{BB,BS}$	14.8 W [25]	Power consumption of baseband digital signal processing in BS
$p_{BB,RN}$	1.5 W [25]	Power consumption of baseband digital signal processing in relay
$p_{ss,BS}$	10.9 W [25]	Power consumption of the small signal transceiver in BS
$p_{ss,RN}$	0.7 W [25]	Power consumption of the small signal transceiver in relay
$\theta_{DC,BS}$	6% [25]	Loss factor of DC-DC power supply in BS
$\theta_{DC,RN}$	8% [25]	Loss factor of DC-DC power supply in relay
$\theta_{MS,BS}$	7% [25]	Loss factor of main supply in BS
$\theta_{MS,RN}$	10% [25]	Loss factor of main supply in RN
$\theta_{cooling,BS}$	9% [25]	Loss factor of cooling in BS
$\theta_{cooling,RN}$	0% [25]	Loss factor of cooling in RN
p_{idle}	0.5 W [27]	Power consumption of in UE RRC idle mode
p_{con}	1.53 W [27]	Power consumption of in UE RRC connected mode
p_{Tx}	0.42 W [27]	Base consumption power of UE when Tx chains active
p_{Rx}	0.55 W [27]	Base consumption power of UE when Rx chains active
p_{Tx+Rx}	0.16 W [27]	Base consumption power of UE when both Tx and Rx are active
p_{TxBB}	2.13 W [27]	Power consumption of the UE baseband part in Tx chains
p_{RxBB}	2.05 W [27]	Power consumption of the UE baseband part in Rx chains

TABLE III
SIMULATION PARAMETERS CORRESPONDING TO THE THEORETICAL DERIVATION

Symbols	Values
Bandwidth B	10 MHz
Variance of noise N_0	-174 dBm/Hz
Frequency of the carrier f_c	1.9 GHz
Distance between BS and UE D	1000 m
Path loss exponent α	4.5 (urban macrocells) [24]
Reference distance d_0	10 m
Path loss coefficient τ_0	1.5788×10^{-6}

τ_0 is set to be the free-space path loss at distance d_0 [24] and is calculated by

$$\tau_0 = \left(\frac{c}{f_c 4\pi d_0}\right)^2 \tag{29}$$

where f_c is the carrier frequency, $c = 3\times10^8$ m/s is the velocity of light, and $d_0 = 10$ m is the reference distance.

Here, we choose the urban macrocell scenario with $\alpha = 4.5$. When small-scale fading is added, we assume that the small-scale fading obeys Rician distribution, the multipath delay profiles obey the Extended Pedestrian A (EPA) model in 3GPP specification 36.104 [31], and the maximum Doppler frequency f_D is 5 Hz. Furthermore, according to the 3GPP specification 36.814 [32], we investigate the optimal relay deployment for the LTE system, whose parameters for the line-of-sight (LOS) path loss, lognormal shadow fading, and Rician small-scale fading are listed in Table IV.

TABLE IV
SIMULATION PARAMETERS FOR LTE SYSTEM

Symbols	Values
Scenario	Case 3 Rural outdoor relay [32]
Inter-site distance (ISD)	1732 m
Bandwidth B	10 MHz
Variance of noise N_0	-174 dBm/Hz
Frequency of the carrier f_c	2.0 GHz
Small scale fading	Rician fading with EPA model [31]
Maximum Doppler frequency	5 Hz
Lognormal shadowing standard derivation σ_{ls} from BS to relay	6 dB
Lognormal shadowing standard derivation σ_{ls} from Relay to UE	10 dB
Path loss from BS to relay for LOS propagation	$100.7 + 23.5\log_{10}(\frac{d_{BS\to RN}}{1000})$
Path loss from Relay to UE for LOS propagation	$103.8 + 20.9\log_{10}(\frac{d_{RN\to UE}}{1000}))$

B. Simulation Results Corresponding to Theoretical Analysis

Figs. 3–7 show that the theoretical results (solid lines) coincide with the numerical simulation results (dash lines), where the numerical simulation results are obtained by using MATLAB to solve the optimization problem in (11). That is to say, Figs. 3–7 validate the correctness of the closed-form expressions for the optimal relay deployment $1/(1+g_{\rm opt})$ and the relative ECI $\eta_{\rm ECI}^{\rm opt}$. Furthermore, the relationships between $1/(1+g_{\rm opt})$ and $\eta_{\rm ECI}^{\rm opt}$ and path loss exponent α, rate ratio β, and spectral efficiency $\eta_{\rm se}$ are analyzed as follows.

1) $1/(1+g_{\rm opt})$ and $\eta_{\rm ECI}^{\rm opt}$ Versus α: As shown in Fig. 3(a) and (b), both $1/(1+g_{\rm opt})$ and $\eta_{\rm ECI}^{\rm opt}$ are increasing functions of α, which coincides with the analysis in the remarks after Theorems 1–3. More specifically, Fig. 3(a) indicates that in bad channel conditions (heavy path loss), the RN should be deployed much farther from the BS than that under good channel conditions (small path loss). In other words, in bad channel conditions, it is possible to improve the energy efficiency while enlarging the cell coverage. However, it will be challenging to extend the cell coverage and enhance the energy efficiency simultaneously under good channel conditions. These two observations can be explained by the fact that $1/(1+g_{\rm opt})$ is an increasing function of α.

Fig. 3(a) shows that, among these three relay transmission schemes, the RN should be deployed the farthest from the BS in the 3TS scheme, whereas the RN should be deployed nearest to the BS in the 4TS scheme. Fig. 3(b) shows that when $\beta = 0.4$ and $\eta_{\rm se} = 10$, the 2TS scheme is the most energy-efficient scheme, whereas the 4TS scheme is the least energy-efficient scheme, i.e., $\eta_{\rm ECI,4TS}^{\rm opt} > \eta_{\rm ECI,3TS}^{\rm opt} > \eta_{\rm ECI,2TS}^{\rm opt}$. This result can be explained by the expressions for the energy efficiencies in (14), (19), and (26), respectively. Specifically, when the energy efficiency $\eta_{\rm se}$ is large, the values of the coefficients in (14), (19), and (26) are mainly decided by the exponential entries $\mu_1 = 2^{4\beta\eta_{\rm se}}$ and $\mu_2 = 2^{4(1-\beta)\eta_{\rm se}}$ in (15), $\mu_3 = 2^{3\beta\eta_{\rm se}}$ and $\mu_4 = 2^{3(1-\beta)\eta_{\rm se}}$ in (21), and $\mu_5 = 2^{2\beta\eta_{\rm se}}$ and $\mu_6 = 2^{2(1-\beta)\eta_{\rm se}}$ in (28), respectively.

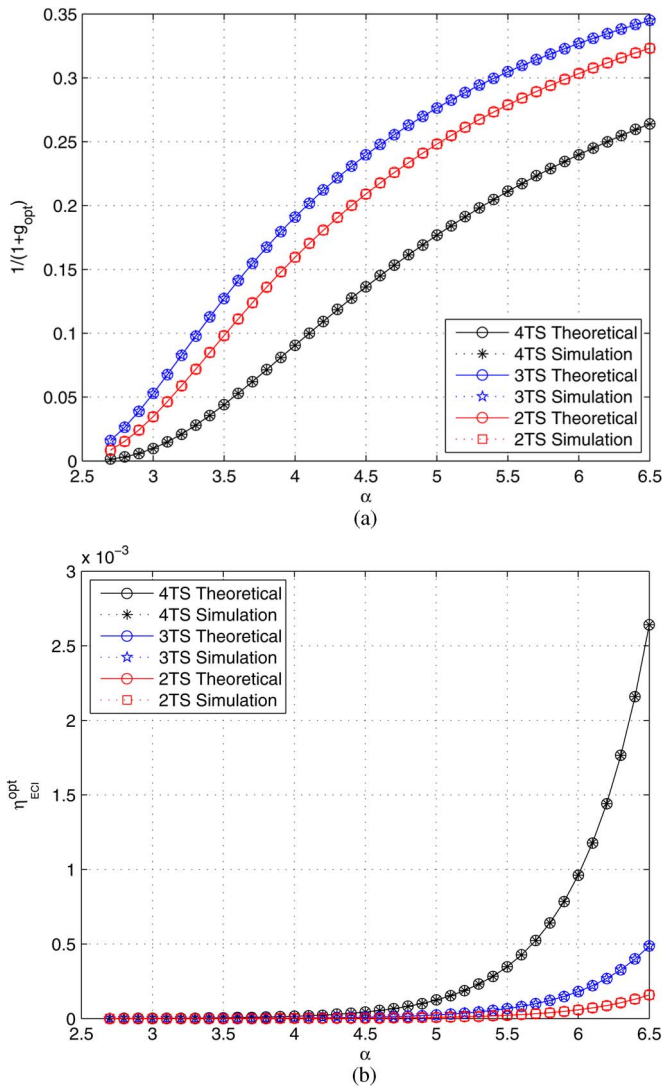

Fig. 3. Optimal relay deployment $1/(1+g_{\rm opt})$ versus path loss exponent α, when $\beta = 0.4$ and $\eta_{\rm se} = 10$.

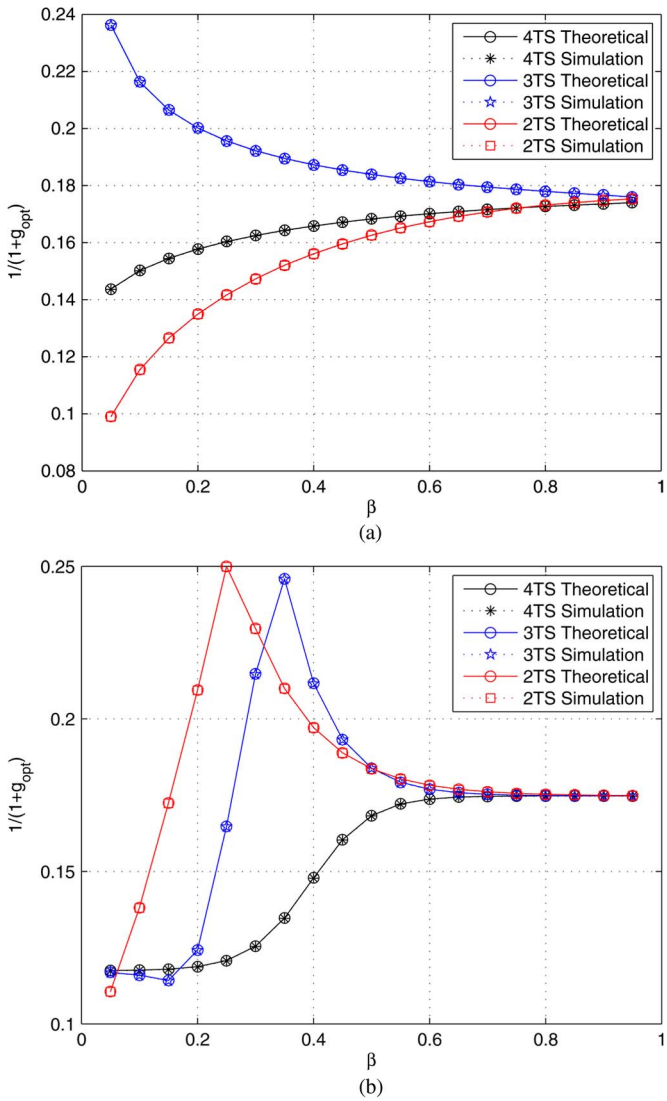

Fig. 4. Optimal relay deployment $1/(1+g_{\rm opt})$ versus rate ratio β at typical values of spectral efficiency $\eta_{\rm se}$ when $\alpha = 4.5$. (a) $\eta_{\rm se} = 1$. (b) $\eta_{\rm se} = 7$.

2) $1/(1+g_{\rm opt})$ and $\eta_{\rm ECI}^{\rm opt}$ Versus β: Fig. 4(a) and (b) shows the trends of the optimal relay deployment $1/(1+g_{\rm opt})$ with the increase in rate ratio β when $\eta_{\rm se} = 1$ and $\eta_{\rm se} = 7$, respectively. Fig. 4 shows that the value of $\eta_{\rm se}$ also has an impact on the trend of $1/(1+g_{\rm opt})$ with respect to β. When the downlink rate is greater than the uplink rate ($\beta > 0.5$), the optimal relay deployments for these three different schemes are almost the same. The reason for this result is that when $\beta > 0.5$, the expressions for the ECI for 4TS, 3TS, and 2TS are (14), $f_{3{\rm TS},1}(g)$ in (20), and $f_{2{\rm TS},1}(g)$ in (27), respectively, whose values are almost the same when $\beta > 0.5$. However, when the downlink rate is smaller than the uplink rate ($\beta < 0.5$), these three schemes have different trends. The different trends with respect to β and discontinuous points of 3TS and 2TS schemes in Fig. 4(b) are due to the piecewise functions in (17) and (23), respectively.

Fig. 5(a) and (b) shows the trends of the ECI at the optimal relay deployment $\eta_{\rm ECI}^{\rm opt}$ with the increase in β when $\eta_{\rm se} = 1$ and $\eta_{\rm se} = 7$, respectively. Fig. 5(b) shows that when the spectral efficiency is high, the 2TS scheme is the most energy efficient, whereas the 4TS scheme is the least energy efficient, which coincides with the result in Fig. 3(b) for the same reason. On the contrary, Fig. 5(a) shows that when the spectral efficiency is low, the 4TS scheme is the most energy efficient, whereas the 2TS scheme is the least energy efficient. This is due to the fact that when $\eta_{\rm se}$ is small, the numbers 4, 3, and 2 in the denominators of the coefficients in (15), (21), and (28) mainly decide the values of $\eta_{\rm ECI,4TS}^{\rm opt}$, $\eta_{\rm ECI,3TS}^{\rm opt}$, and $\eta_{\rm ECI,2TS}^{\rm opt}$, respectively.

3) $1/(1+g_{\rm opt})$ and $\eta_{\rm ECI}^{\rm opt}$ Versus $\eta_{\rm se}$: Fig. 6(a) and (b) shows the trends of the optimal relay deployment $1/(1+g_{\rm opt})$ with the increase in spectral efficiency $\eta_{\rm se}$ when $\beta = 0.2$ and $\beta = 0.7$, respectively. Fig. 6 shows that the value of β affects the trends of $1/(1+g_{\rm opt})$ with respect to $\eta_{\rm se}$. Furthermore, when $\eta_{\rm se}$ is large enough, the optimal relay deployments for these three schemes are almost the same. However, when $\eta_{\rm se}$ is small, these three schemes have different trends. This result is very similar to that in Fig. 4(b) with the same reason.

Fig. 7(a) and (b) demonstrates the trends of the ECI at the optimal relay deployment $\eta_{\rm ECI}^{\rm opt}$ with the increase in spectral

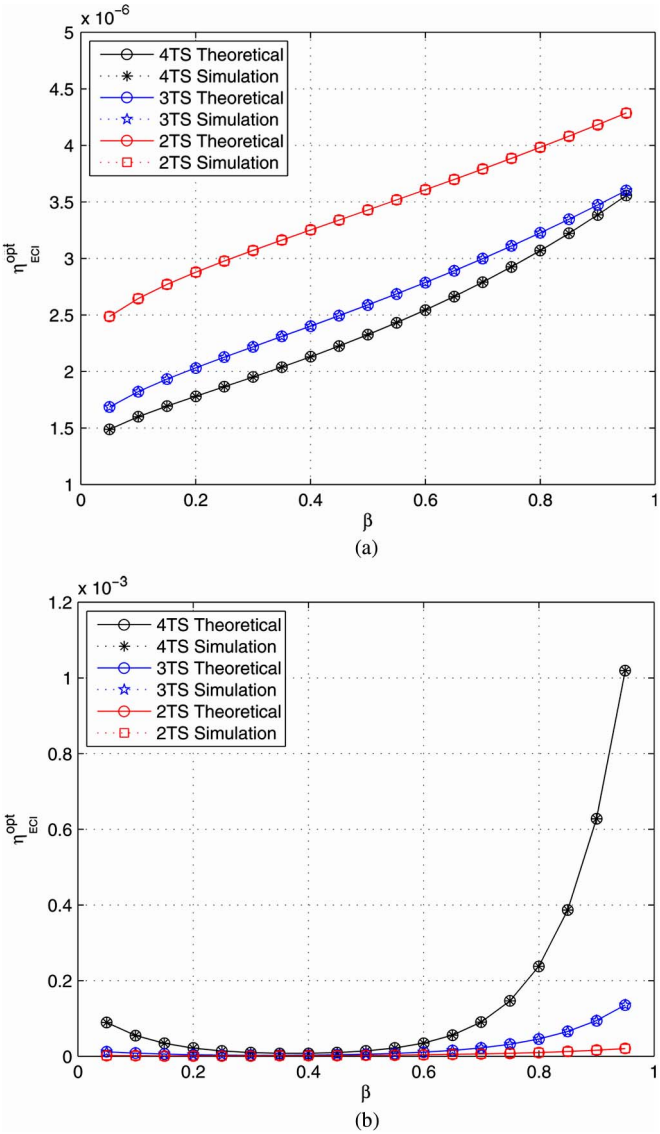

Fig. 5. ECI at the optimal relay deployment $\eta_{\mathrm{ECI}}^{\mathrm{opt}}$ versus rate ratio β at typical values of spectral efficiency η_{se} when $\alpha = 4.5$. (a) $\eta_{\mathrm{se}} = 1$. (b) $\eta_{\mathrm{se}} = 7$.

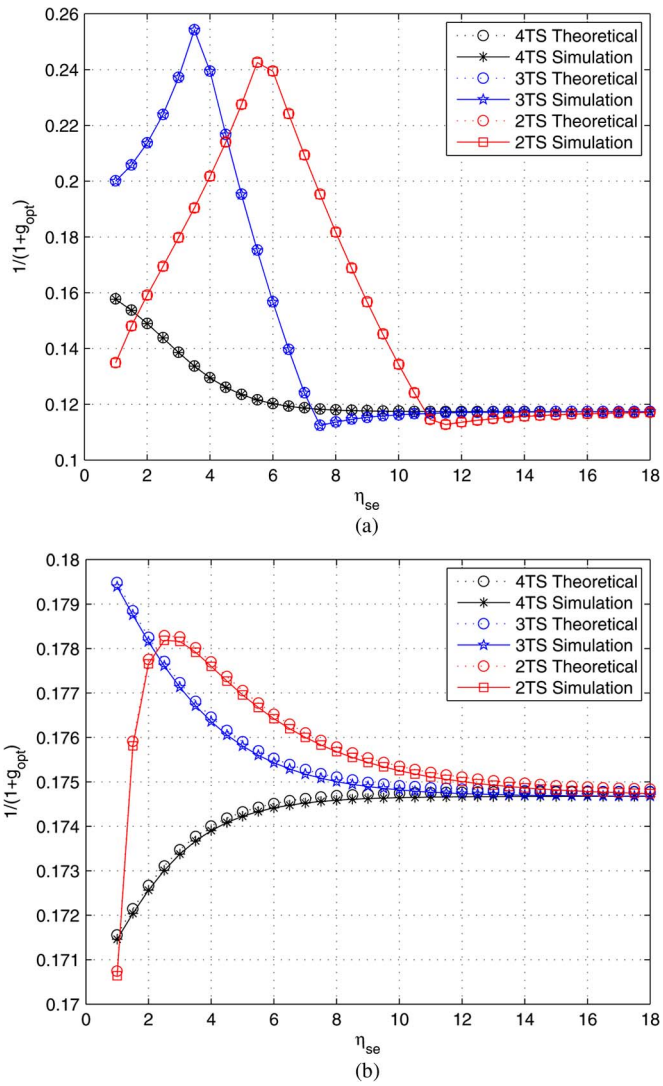

Fig. 6. Optimal relay deployment $1/(1+g_{\mathrm{opt}})$ versus spectral efficiency η_{se} at typical values of rate ratio β when $\alpha = 4.5$. (a) $\beta = 0.2$. (b) $\beta = 0.7$.

efficiency η_{se} when $\beta = 0.2$ and $\beta = 0.7$, respectively. Fig. 7(a) and (b) shows that when η_{se} is large enough, the 2TS scheme is the most energy efficient, whereas the 4TS scheme is the least energy efficient, which coincides with the result in Fig. 3(b).

4) $1/(1+g_{\mathrm{opt}})$ Versus β and η_{se}: Fig. 8 comprehensively describes the trends of $1/(1+g_{\mathrm{opt}})$ with the increases in β and η_{se}. Fig. 8(a) shows that the optimal deployment of the 4TS scheme $1/(1+g_{4\mathrm{TS,opt}})$ increases with β when $0.2 < \beta < 0.4$, whereas $1/(1+g_{4\mathrm{TS,opt}})$ remains as a constant at other regions with the increase in β and η_{se}. Similarly, both $1/(1+g_{3\mathrm{TS,opt}})$ and $1/(1+g_{2\mathrm{TS,opt}})$ have peaks in the region $0.2 < \beta < 0.4$, and the peaks increase with the increases in η_{se}. The different trends with respect to β and η_{se} in Fig. 8(b) and (c) are due to the piecewise functions in (17) and (23). Moreover, when the downlink rate is much greater or much smaller than the uplink rate, the optimal relay deployments for these three schemes are almost the same. Otherwise, these three schemes have different optimal relay deployments.

C. Nonideal PA Versus Ideal PA

Figs. 9 and 10 demonstrate the impacts of the nonideal PA in comparison with that of the ideal PA with respect to α and β, respectively. Both Figs. 9(a) and 10(a) show that the optimal relay deployment with the nonideal PA is much closer to the BS in comparison with that of the ideal PA, which is around the middle point of the BS and the relay. This phenomenon can be explained by the closed-form expressions for the optimal relay deployment with the ideal PA and the nonideal PA. As shown in (13), (17), and (23), the expressions for g_{opt} with the nonideal PA can be generalized as

$$g_{\mathrm{opt,non}} = \left(\frac{A_{ij}}{B_{ij}}\right)^{\frac{2}{\alpha-2}} \tag{30}$$

where A_{ij} and B_{ij} are the coefficients defined in (15), (21), and (28). Similarly, we can obtain the generalized expression for g_{opt} with the ideal PA as

$$g_{\mathrm{opt,ideal}} = \left(\frac{A'_{ij}}{B'_{ij}}\right)^{\frac{1}{\alpha-1}} \tag{31}$$

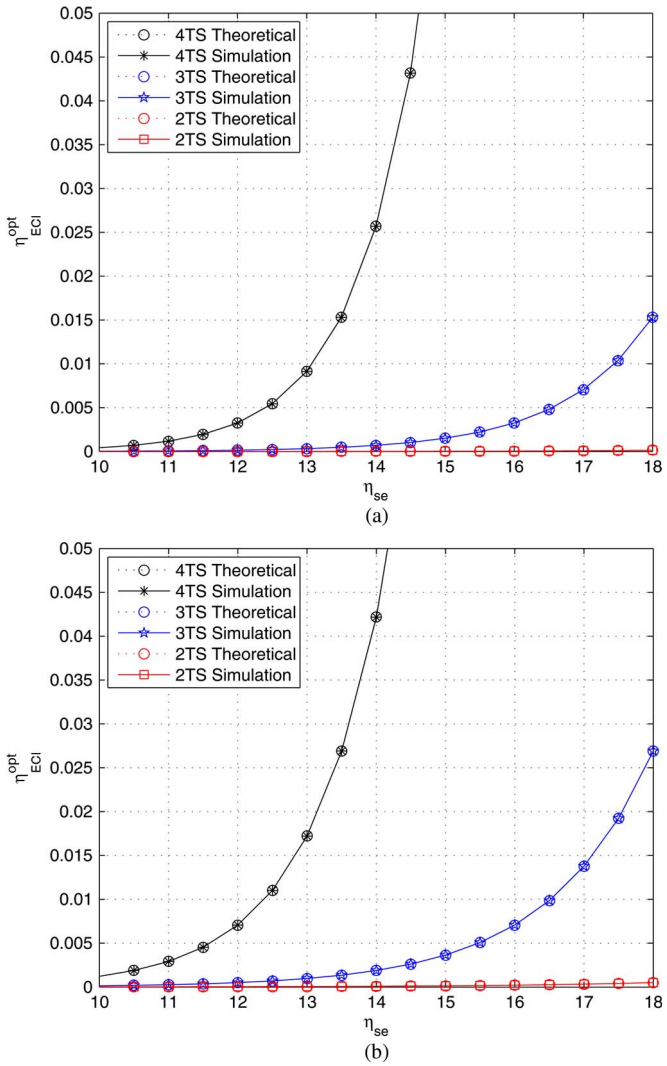

Fig. 7. ECI at the optimal relay deployment $\eta_{\mathrm{ECI}}^{\mathrm{opt}}$ versus spectral efficiency η_{se} at typical values of rate ratio β when $\alpha = 4.5$. (a) $\beta = 0.2$. (b) $\beta = 0.7$.

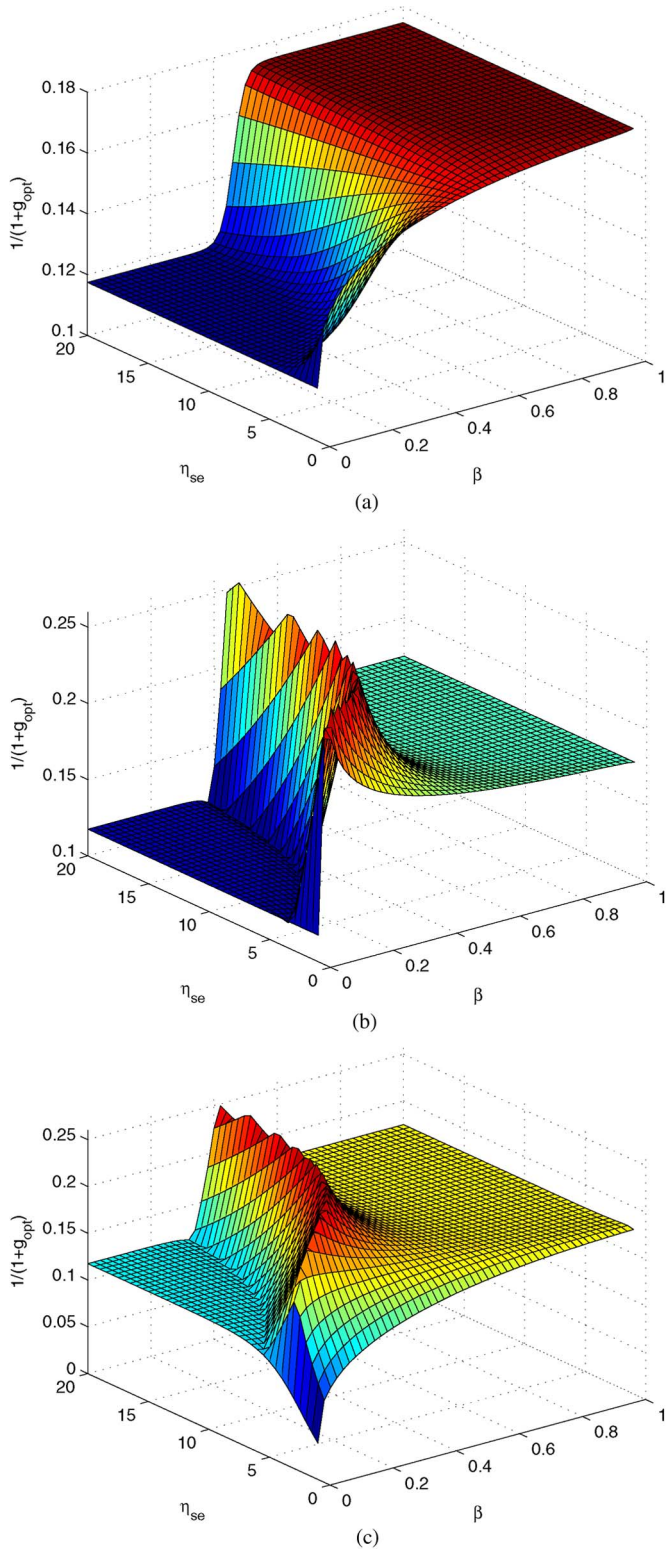

Fig. 8. Optimal relay deployment $1/(1+g_{\mathrm{opt}})$ versus rate ratio β and spectral efficiency η_{se} when $\alpha = 4.5$. (a) 4TS scheme. (b) 3TS scheme. (c) 2TS scheme.

where A'_{ij} and B'_{ij} are similar coefficients as A_{ij} and B_{ij}. As stated in the remarks after Theorems 1–3, the base of g_{opt} is greater than 1; hence, we have $g_{\mathrm{opt,non}} > g_{\mathrm{opt,ideal}}$ and $1/(1+g_{\mathrm{opt,non}}) < 1/(1+g_{\mathrm{opt,ideal}})$ when $\alpha > 2$. Moreover, both Figs. 9(b) and 10(b) indicate that, due to the different PA models, the ECI at the optimal relay deployment with the nonideal PA is much smaller than that with the ideal PA.

D. Optimal Relay Deployment in More Practical Scenarios

1) Adding Small-Scale Fading: Figs. 11 and 12 present the impacts of small-scale fading in comparison with those without small-scale fading with respect to α and β, respectively. Fig. 11(a) shows that when the path loss is very small, the RN in all these three schemes should be deployed farther from the BS when considering small-scale fading than that without small-scale fading. On the contrary, both Figs. 11(a) and 12(a) show that when the path loss is large, the RN should be deployed nearer to the BS when considering small-scale fading than that without small-scale fading. Both Figs. 11(b) and 12(b) show that when considering small-scale fading, the energy consumption at the optimal relay deployment is larger than that without small-scale fading. The reason for this phenomenon is that with small-scale fading, the channel capacity becomes smaller than that without small-scale fading, that is to say, the transmitter needs larger power to achieve the same transmission rate.

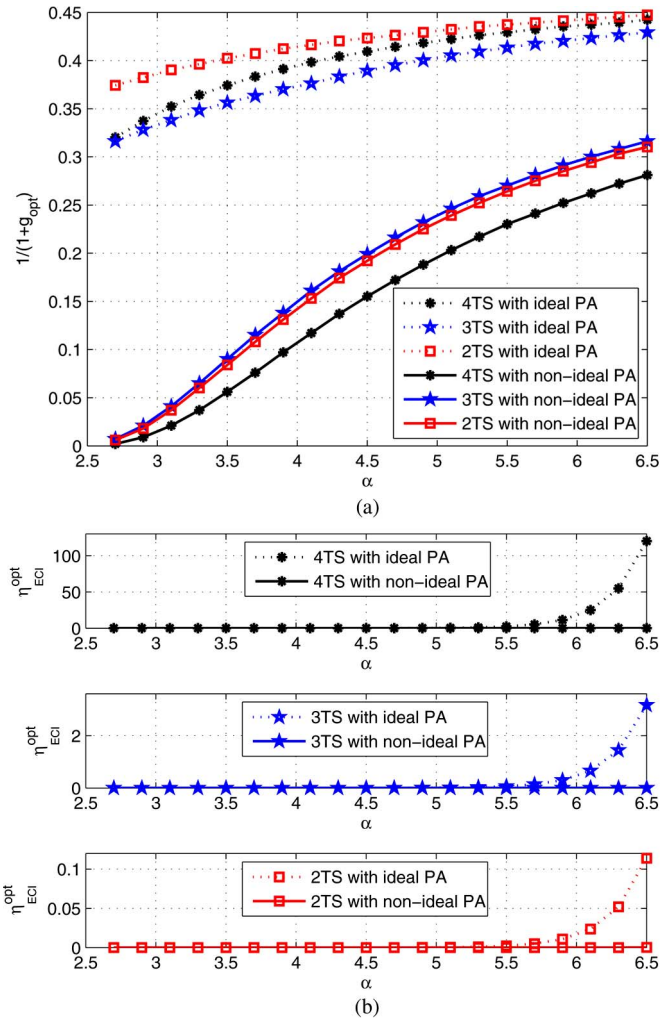

Fig. 9. Comparison with the scenario of the ideal PA with respect to α when $\beta = 0.45$ and $\eta_{\rm se} = 10$. (a) Optimal relay deployment $1/(1 + g_{\rm opt})$. (b) ECI at the optimal relay deployment $\eta_{\rm ECI}^{\rm opt}$.

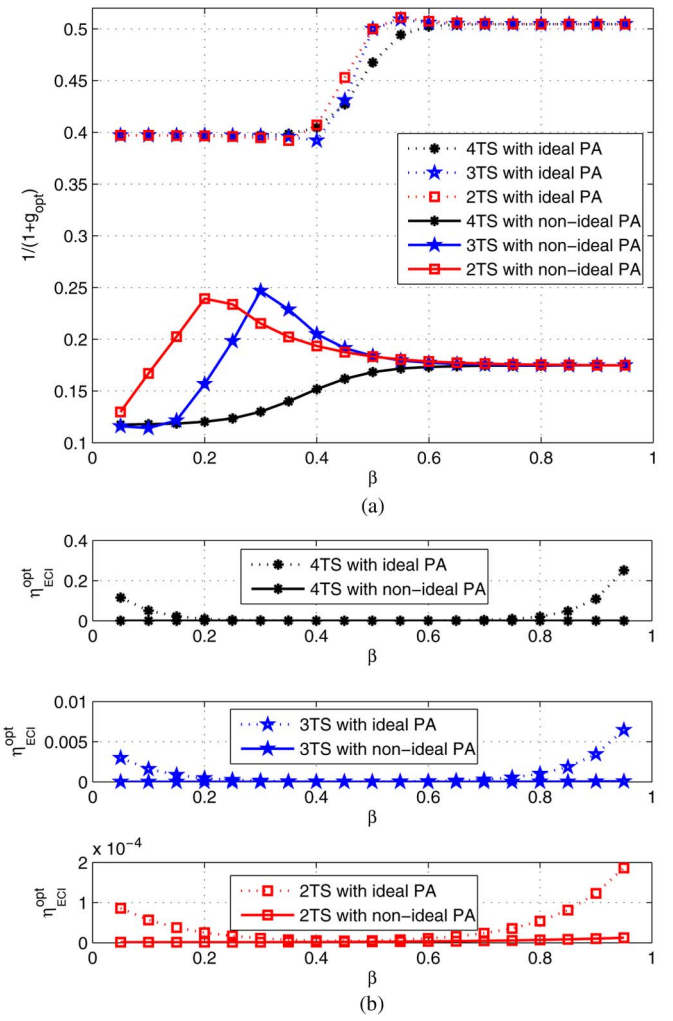

Fig. 10. Comparison with the scenario of the ideal PA with respect to β when $\alpha = 4.5$ and $\eta_{\rm se} = 6$. (a) Optimal relay deployment $1/(1 + g_{\rm opt})$. (b) ECI at the optimal relay deployment $\eta_{\rm ECI}^{\rm opt}$.

LTE Outdoor Rural Scenario: Fig. 13 shows the optimal relay deployment $1/(1 + g_{\rm opt})$ and the relative ECI $\eta_{\rm ECI}^{\rm opt}$ for the LTE system in a rural outdoor scenario with LOS propagation when $\eta_{\rm se} = 10$. The simulation results in Fig. 13(a) validate the given analysis with respect to α, where the equivalent path loss exponent α is 2.35 from the BS to the relay and 2.09 from the relay to the UE. Fig. 13(b) indicates that it may not be easy to achieve the optimal energy efficiency and extend the cell coverage simultaneously in this good LTE channel condition with LOS propagation, where we can only make a tradeoff between the cell coverage and the energy efficiency. Fig. 13(b) shows that the 2TS scheme is the most energy efficient, whereas the 4TS scheme is the least energy efficient under the high-spectral-efficiency scenario, which coincides with the results in Fig. 3(b), Fig. 5(b), and Fig. 7.

In summary, we obtain the following important conclusions for the optimal energy-efficient relay deployment and the corresponding energy efficiency.

- First, it is possible to achieve the optimal energy efficiency and enlarge the cell coverage simultaneously under bad channel conditions, e.g., heavy path loss. However, it is challenging to realize the given two goals at the same time under good channel conditions, e.g., small path loss.
- Second, under an asymmetric traffic condition, when the downlink rate is larger than the uplink rate, the optimal relay deployments for 4TS, 3TS, and 2TS schemes have similar trends. However, when the downlink rate is smaller than the uplink rate, the optimal relay deployments for the three schemes have different trends.
- Third, when the spectral efficiency is high, the 2TS scheme is the most energy efficient at the optimal relay deployment in comparison with the 3TS and 4TS schemes. On the contrary, when the spectral efficiency is low, the 4TS scheme is the most energy efficient at the optimal relay deployment among these three schemes.
- Fourth, when considering the nonideal PA, the RN should be deployed closer to the BS than that with the ideal PA. The energy efficiencies at the optimal relay deployment for these three schemes with the nonideal PA are higher than those with the ideal PA.
- Fifth, the impact of small-scale fading depends on the value of path loss. Specifically, when the path loss is very

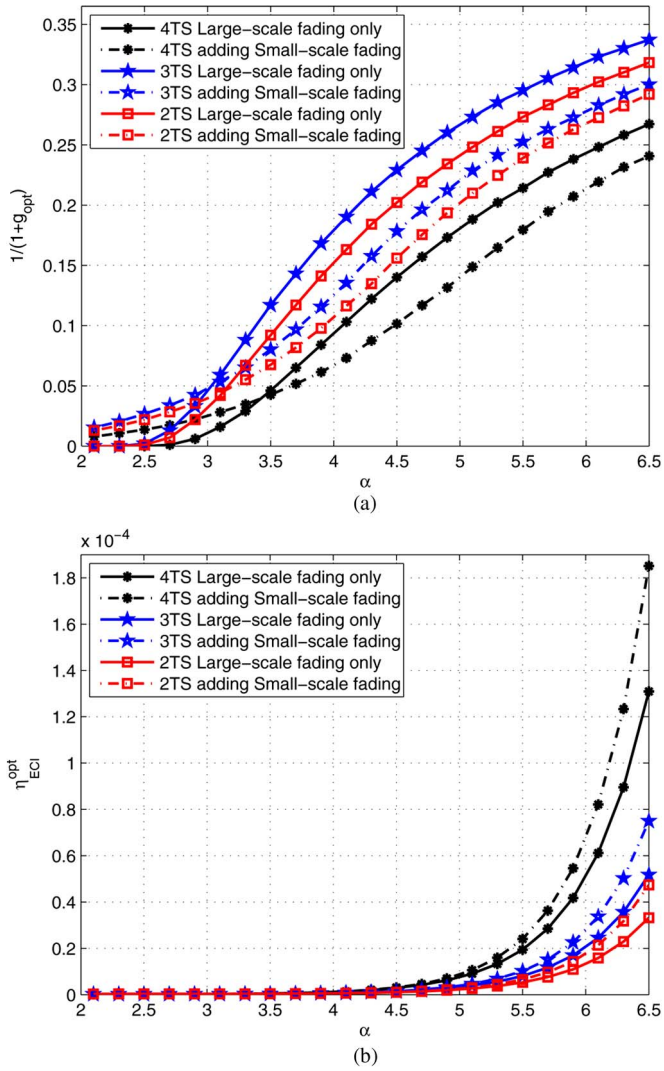

Fig. 11. Considering small-scale fading with respect to α when $\beta = 0.35$ and $\eta_{\rm se} = 6$. (a) Optimal relay deployment $1/(1 + g_{\rm opt})$. (b) ECI at the optimal relay deployment $\eta_{\rm ECI}^{\rm opt}$.

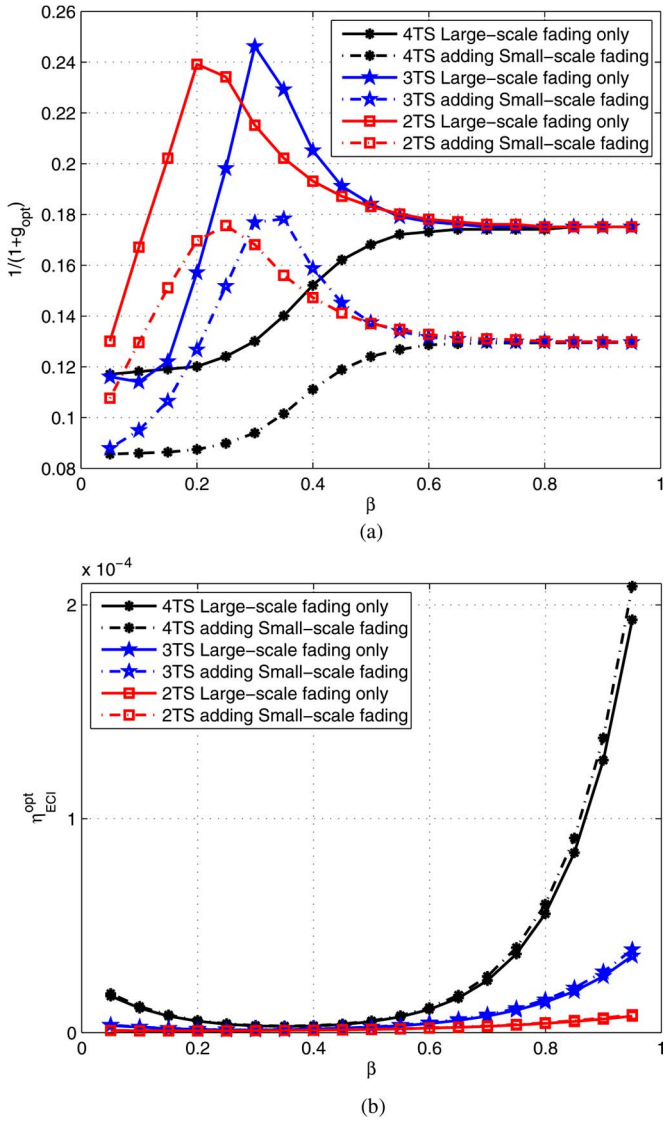

Fig. 12. Considering small-scale fading with respect to β when $\alpha = 4.5$ and $\eta_{\rm se} = 6$. (a) Optimal relay deployment $1/(1 + g_{\rm opt})$. (b) ECI at the optimal relay deployment $\eta_{\rm ECI}^{\rm opt}$.

small, the RN should be deployed farther from the BS than that without small-scale fading. On the contrary, when the path loss is large, the RN should be deployed closer to the BS than that without small-scale fading. Moreover, compared with the scenario without small-scale fading, the transmission nodes need to consume more energy to overcome the small-scale fading.

- Finally, the simulation results for the LTE system validate the analysis results with respect to the channel condition. Specifically, it may be hard to extend the cell coverage and achieve the optimal energy efficiency simultaneously due to the good channel condition with LOS propagation, where we can only make a tradeoff between the cell coverage and the energy efficiency.

V. Conclusion

In this paper, we have investigated the optimal energy-efficient relay deployments for the 2TS, 3TS, and 4TS bidirectional relay transmission schemes. Via the derived closed-form expressions for the optimal relay deployments and the relative ECI and numerical simulations, we obtain the following important conclusions. First, it is possible to achieve the optimal energy efficiency and extend the cell coverage simultaneously in bad channel conditions, but it is challenging in good channel conditions. Second, under asymmetric traffic conditions, particularly when the downlink rate is larger than the uplink rate, all the aforementioned three schemes have almost the same optimal relay deployment, but the 2TS scheme has the best energy efficiency when the spectral efficiency is high. Third, the RN should be deployed nearer to the BS with the nonideal PA than that with the ideal PA. Finally, the impact of small-scale fading depends on the value of path loss. Compared with the scenario without small-scale fading, the transmission nodes need to consume more energy to overcome the small-scale fading. In future work, we will theoretically investigate the optimal energy-efficient relay deployment in more practical wireless channels, e.g., the scenario with small-scale fading.

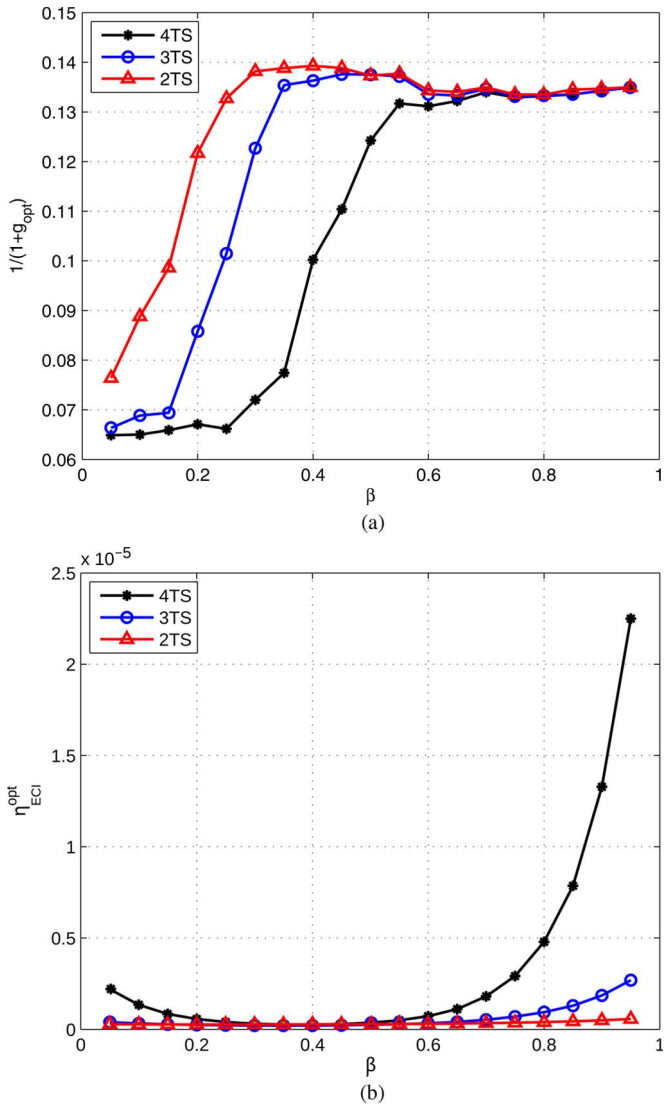

Fig. 13. LTE outdoor rural scenario with LOS propagation and $\eta_{\text{se}} = 10$. (a) Optimal relay deployment $1/(1+g_{\text{opt}})$. (b) ECI at the optimal relay deployment $\eta_{\text{ECI}}^{\text{opt}}$.

APPENDIX A
PROOF OF THEOREM 1

For the 4TS transmission scheme with the DF relay strategy, the achievable transmission rate in each direction is decided by the weakest link of the transmission path, i.e.,

$$\begin{aligned} &R_{\text{BS}\to\text{UE},4\text{TS}} \\ &\quad = \mathbf{min}\left\{\frac{1}{4}B\log_2\left(1+\frac{|h_{\text{BS}\to\text{RN}}|^2 P_{\text{out,BS}}}{\sigma^2}\right)\right. \\ &\qquad \left.\frac{1}{4}B\log_2\left(1+\frac{|h_{\text{RN}\to\text{UE}}|^2 P_{\text{out,RN}_1}}{\sigma^2}\right)\right\} \end{aligned} \tag{32}$$

$$\begin{aligned} &R_{\text{UE}\to\text{BS},4\text{TS}} \\ &\quad = \mathbf{min}\left\{\frac{1}{4}B\log_2\left(1+\frac{|h_{\text{UE}\to\text{RN}}|^2 P_{\text{out,UE}}}{\sigma^2}\right)\right. \\ &\qquad \left.\frac{1}{4}B\log_2\left(1+\frac{|h_{\text{RN}\to\text{BS}}|^2 P_{\text{out,RN}_2}}{\sigma^2}\right)\right\} \end{aligned} \tag{33}$$

where $P_{\text{out,RN}_1}$ denotes the transmit output power of the relay station in the second transmission time slot, and $P_{\text{out,RN}_2}$ denotes the transmit output power of the relay station in the fourth transmission time slot. The pre-log factor 1/4 is due to the 4TS required in this transmission scheme.

Let T_s denote one-time-slot duration, according to the power consumption model in (7) and (8), the sum of the total power consumption of the BS, the relay, and the UE in the 4TS scheme is

$$\begin{aligned} P_{s,4\text{TS}} &= \frac{1}{4}(P_{\text{total,BS}} + P_{\text{total,RN}_1} + P_{\text{total,UE}} + P_{\text{total,RN}_2}) \\ &= \frac{1}{4}\left(\rho_{\text{BS}}\gamma_{\text{BS}}\sqrt{P_{\text{out,BS}}} + \rho_{\text{UE}}\overline{m_{\text{idle}}}\sqrt{P_{\text{out,UE}}}\right. \\ &\qquad \left. + \rho_{\text{RN}}\gamma_{\text{RN}}\left(\sqrt{P_{\text{out,RN}_1}} + \sqrt{P_{\text{out,RN}_2}}\right)\right) \\ &\quad + C_{4\text{TS}} \end{aligned} \tag{34}$$

where $C_{4\text{TS}} = (P_{C,\text{BS}} + P_{C,\text{UE}} + 2P_{C,\text{RN}})/4$ is the sum of the constant power consumed by other parts beside the RF part in the BS, the relay, and the UE in the 4TS transmission scheme.

Then, the optimization problem in (11) for the 4TS scheme turns into

$$\begin{aligned} \min_{g} \quad & \eta_{\text{ECI},4\text{TS}} = \frac{P_{s,4\text{TS}}}{R_s} \\ \text{s.t.} \quad & R_{\text{BS}\to\text{UE},4\text{TS}} = \beta R_s \\ & R_{\text{UE}\to\text{BS},4\text{TS}} = (1-\beta)R_s. \end{aligned} \tag{35}$$

Based on the expressions for $R_{\text{BS}\to\text{UE},4\text{TS}}$ and $R_{\text{UE}\to\text{BS},4\text{TS}}$ in (32) and (33), to minimize the total power consumption, the constraints are satisfied only if the uplink transmission rate is equal to the downlink transmission rate. That is to say, the two parts of the min functions in (32) and (33) are equal. Then, according to (2) and (4), the expressions for $P_{\text{out,BS}}$, $P_{\text{out,RN}_1}$, $P_{\text{out,UE}}$, and $P_{\text{out,RN}_2}$ can be written as follows:

$$\begin{aligned} P_{\text{out,BS}} &= A_{1,1}^2\left(\frac{1}{1+g}\right)^{\alpha}, \quad P_{\text{out,RN}_1} = A_{1,1}^2\left(\frac{g}{1+g}\right)^{\alpha} \\ P_{\text{out,UE}} &= B_{1,1}^2\left(\frac{g}{1+g}\right)^{\alpha}, \quad P_{\text{out,RN}_2} = B_{1,1}^2\left(\frac{1}{1+g}\right)^{\alpha} \end{aligned} \tag{36}$$

where the values of the constants are expressed as follows:

$$\begin{aligned} A_{1,1}^2 &= \frac{\sigma^2}{\tau_0 d_0^{\alpha}} D^{\alpha}\left(2^{\frac{4\beta R_s}{B}} - 1\right) \\ B_{1,1}^2 &= \frac{\sigma^2}{\tau_0 d_0^{\alpha}} D^{\alpha}\left(2^{\frac{4(1-\beta)R_s}{B}} - 1\right). \end{aligned} \tag{37}$$

Substitute (36) into the optimization objective function in (35), we have

$$\begin{aligned} \eta_{\text{ECI},4\text{TS}}(g) &= f_{4\text{TS}}(g) \\ &= A_{1,2}\left(\frac{1}{1+g}\right)^{\frac{\alpha}{2}} + B_{1,2}\left(\frac{g}{1+g}\right)^{\frac{\alpha}{2}} + \frac{C_{4\text{TS}}}{R_s} \end{aligned} \tag{38}$$

where the expressions for $A_{1,2}$ and $B_{1,2}$ are

$$A_{1,2} = \frac{1}{4R_s}(\rho_{\mathrm{BS}}\gamma_{\mathrm{BS}}A_{1,1} + \rho_{\mathrm{RN}}\gamma_{\mathrm{RN}}B_{1,1})$$
$$B_{1,2} = \frac{1}{4R_s}(\rho_{\mathrm{UE}}\overline{m_{\mathrm{idle}}}B_{1,1} + \rho_{\mathrm{RN}}\gamma_{\mathrm{RN}}A_{1,1}). \quad (39)$$

The optimal relay deployment will be achieved at the solution to $\partial f_{4\mathrm{TS}}(g)/\partial g = 0$, i.e.,

$$g_{4\mathrm{TS,opt}} = \left(\frac{A_{1,2}}{B_{1,2}}\right)^{\frac{2}{\alpha-2}}. \quad (40)$$

Therefore, the optimal relay deployment for the 4TS transmission is

$$d^{4\mathrm{TS}}_{\mathrm{RN}\to\mathrm{UE}} = \left(\frac{A_{1,2}}{B_{1,2}}\right)^{\frac{2}{\alpha-2}} d^{4\mathrm{TS}}_{\mathrm{BS}\to\mathrm{RN}}. \quad (41)$$

Substitute (37) into (39), we can obtain the explicit expressions for $A_{1,2}$ and $B_{1,2}$ as in (15). Then, after substituting (15) into (40), we can get the explicit expression for the optimal relay deployment of the 4TS transmission in (13). ■

Appendix B
Proof of Theorem 2

Similar to the 4TS scheme, the achievable rate for the 3TS scheme with the DF protocol is decided by the weakest link of each direction. Thus, we have

$$R_{\mathrm{BS}\to\mathrm{UE},3\mathrm{TS}} = \mathbf{min}\left\{\frac{1}{3}B\log_2\left(1+\frac{|h_{\mathrm{BS}\to\mathrm{RN}}|^2P_{\mathrm{out,BS}}}{\sigma^2}\right), \frac{1}{3}B\log_2\left(1+\frac{|h_{\mathrm{RN}\to\mathrm{UE}}|^2P_{\mathrm{out,RN}}}{\sigma^2}\right)\right\} \quad (42)$$

$$R_{\mathrm{UE}\to\mathrm{BS},3\mathrm{TS}} = \mathbf{min}\left\{\frac{1}{3}B\log_2\left(1+\frac{|h_{\mathrm{UE}\to\mathrm{RN}}|^2P_{\mathrm{out,UE}}}{\sigma^2}\right), \frac{1}{3}B\log_2\left(1+\frac{|h_{\mathrm{RN}\to\mathrm{BS}}|^2P_{\mathrm{out,RN}}}{\sigma^2}\right)\right\} \quad (43)$$

where the pre-log factor 1/3 comes from the 3TS required in this transmission scheme. The sum of the total power consumption of the BS, the relay, and the UE in the 3TS scheme is calculated by

$$P_{s,3\mathrm{TS}} = \frac{1}{3}\left(\rho_{\mathrm{BS}}\gamma_{\mathrm{BS}}\sqrt{P_{\mathrm{out,BS}}} + \rho_{\mathrm{UE}}\overline{m_{\mathrm{idle}}}\sqrt{P_{\mathrm{out,UE}}} + \rho_{\mathrm{RN}}\gamma_{\mathrm{RN}}\sqrt{P_{\mathrm{out,RN}}}\right) + C_{3\mathrm{TS}} \quad (44)$$

where $C_{3\mathrm{TS}} = (P_{C,\mathrm{BS}} + P_{C,\mathrm{UE}} + P_{C,\mathrm{RN}})/3$ is the sum of the constant power consumed by other parts beside the RF part in the BS, the relay, and the UE in the 3TS transmission scheme.

Then, the optimization problem in (11) for the 3TS scheme turns into

$$\min_{g} \quad \eta_{\mathrm{ECI},3\mathrm{TS}} = \frac{P_{s,3\mathrm{TS}}}{R_s}$$
$$\text{s.t.} \quad R_{\mathrm{BS}\to\mathrm{UE},3\mathrm{TS}} = \beta R_s$$
$$R_{\mathrm{UE}\to\mathrm{BS},3\mathrm{TS}} = (1-\beta)R_s. \quad (45)$$

Note that both $R_{\mathrm{BS}\to\mathrm{UE},3\mathrm{TS}}$ and $R_{\mathrm{UE}\to\mathrm{BS},3\mathrm{TS}}$ in (42) and (43) rely on the same variable $P_{\mathrm{out,RN}}$; thus, $P_{\mathrm{out,RN}}$ should be larger such that it satisfies both of these two constraints in (45). Thus, we have the expressions for $P_{\mathrm{out,BS}}$, $P_{\mathrm{out,UE}}$, and $P_{\mathrm{out,RN}}$ as follows:

$$P_{\mathrm{out,BS}} = A^2_{2,1}\left(\frac{1}{1+g}\right)^{\alpha}, \quad P_{\mathrm{out,UE}} = B^2_{2,1}\left(\frac{g}{1+g}\right)^{\alpha}$$
$$P_{\mathrm{out,RN}} = \mathbf{max}\left\{A^2_{2,1}\left(\frac{g}{1+g}\right)^{\alpha}, B^2_{2,1}\left(\frac{1}{1+g}\right)^{\alpha}\right\} \quad (46)$$

where the expressions of $A^2_{2,1}$ and $B^2_{2,1}$ are

$$A^2_{2,1} = \frac{\sigma^2}{\tau_0 d_0^{\alpha}}D^{\alpha}\left(2^{\frac{3\beta R_s}{B}} - 1\right),$$
$$B^2_{2,1} = \frac{\sigma^2}{\tau_0 d_0^{\alpha}}D^{\alpha}\left(2^{\frac{3(1-\beta)R_s}{B}} - 1\right). \quad (47)$$

Substitute (46) into the optimization objective function in (45), we have

$$\eta_{\mathrm{ECI},3\mathrm{TS}}(g) = f_{3\mathrm{TS}}(g) = \mathbf{max}\left\{f_{3\mathrm{TS},1}(g), f_{3\mathrm{TS},1}(g)\right\} \quad (48)$$

where the expressions for $f_{3\mathrm{TS},1}(g)$ and $f_{3\mathrm{TS},2}(g)$ are

$$f_{3\mathrm{TS},1}(g) = A_{2,2}\left(\frac{1}{1+g}\right)^{\frac{\alpha}{2}} + B_{2,2}\left(\frac{g}{1+g}\right)^{\frac{\alpha}{2}} + \frac{C_{3\mathrm{TS}}}{R_s} \quad (49)$$

$$f_{3\mathrm{TS},2}(g) = A_{2,3}\left(\frac{1}{1+g}\right)^{\frac{\alpha}{2}} + B_{2,3}\left(\frac{g}{1+g}\right)^{\frac{\alpha}{2}} + \frac{C_{3\mathrm{TS}}}{R_s} \quad (50)$$

where the expressions for $A_{2,2}$, $B_{2,2}$, $A_{2,3}$, and $A_{3,3}$ are

$$A_{2,2} = \frac{1}{3R_s}\rho_{\mathrm{BS}}\gamma_{\mathrm{BS}}A_{2,1}$$
$$B_{2,2} = \frac{1}{3R_s}(\rho_{\mathrm{UE}}\overline{m_{\mathrm{idle}}}B_{2,1} + \rho_{\mathrm{RN}}\gamma_{\mathrm{RN}}A_{2,1})$$
$$A_{2,3} = \frac{1}{3R_s}(\rho_{\mathrm{BS}}\gamma_{\mathrm{BS}}A_{2,1} + \rho_{\mathrm{RN}}\gamma_{\mathrm{RN}}B_{2,1})$$
$$B_{2,3} = \frac{1}{3R_s}\rho_{\mathrm{UE}}\overline{m_{\mathrm{idle}}}B_{2,1}. \quad (51)$$

Let $f_{3\mathrm{TS,dif}}(g)$ denote the difference between $f_{3\mathrm{TS},1}(g)$ and $f_{3\mathrm{TS},2}(g)$, i.e.,

$$f_{3\mathrm{TS,dif}}(g) = f_{3\mathrm{TS},1}(g) - f_{3\mathrm{TS},2}(g)$$
$$= (A_{2,2} - A_{2,3})\left(\frac{1}{1+g}\right)^{\frac{\alpha}{2}} + (B_{2,2} - B_{2,3})\left(\frac{g}{1+g}\right)^{\frac{\alpha}{2}}. \quad (52)$$

Then, the threshold for $f_{3\mathrm{TS}}(g)$ is the solution to $f_{3\mathrm{TS,dif}}(g) = 0$, i.e.,

$$g_{3\mathrm{TS,th}} = \left(\frac{A_{2,3} - A_{2,2}}{B_{2,2} - B_{2,3}}\right)^{\frac{2}{\alpha}}. \tag{53}$$

To decide when $f_{3\mathrm{TS}}(g) = f_{3\mathrm{TS},1}(g)$ and when $f_{3\mathrm{TS}}(g) = f_{3\mathrm{TS},2}(g)$, the derivative of $f_{3\mathrm{TS,dif}}(g)$ with respect to g is calculated as follows:

$$\frac{\partial f_{3\mathrm{TS,dif}}}{\partial g} = (A_{2,3} - A_{2,2})\left(\frac{1}{1+g}\right)^{\frac{\alpha}{2}+1} + (B_{2,2} - B_{2,3})\left(\frac{1}{1+g}\right)^{\frac{\alpha}{2}+1} g^{\frac{\alpha}{2}-1}. \tag{54}$$

From (54), we can conclude that $\partial f_{3\mathrm{TS,dif}}/\partial g > 0$ for all $g > 0$, that is to say, $f_{3\mathrm{TS,dif}}(g)$ is an increasing function. Thus, we have the explicit expression of $f_{3\mathrm{TS}}(g)$ as

$$f_{3\mathrm{TS}}(g) = \begin{cases} f_{3\mathrm{TS},2}(g), & \text{if } g < g_{3\mathrm{TS,th}} \\ f_{3\mathrm{TS},1}(g), & \text{if } g \geq g_{3\mathrm{TS,th}}. \end{cases} \tag{55}$$

Based on (55), we can conclude that the optimal relay deployment will be achieved at the extreme points of $f_{3\mathrm{TS},2}(g)$ and $f_{3\mathrm{TS},1}(g)$ or the threshold $g_{3\mathrm{TS,th}}$. Thus, we have

$$g_{3\mathrm{TS,opt}} = \begin{cases} g_2 = \left(\frac{A_{2,3}}{B_{2,3}}\right)^{\frac{2}{\alpha-2}}, & \text{if } g_2 < g_{3\mathrm{TS,th}} \\ g_1 = \left(\frac{A_{2,2}}{B_{2,2}}\right)^{\frac{2}{\alpha-2}}, & \text{if } g_1 \geq g_{3\mathrm{TS,th}} \\ g_{3\mathrm{TS,th}} = \left(\frac{A_{2,3}-A_{2,2}}{B_{2,2}-B_{2,3}}\right)^{\frac{2}{\alpha}}, & \text{otherwise.} \end{cases} \tag{56}$$

Therefore, the optimal relay deployment for the 3TS scheme is

$$d^{3\mathrm{TS}}_{\mathrm{RN}\to\mathrm{UE}} = g_{3\mathrm{TS,opt}} d^{3\mathrm{TS}}_{\mathrm{BS}\to\mathrm{RN}}. \tag{57}$$

If we substitute (47) into (51), we can get the explicit expressions for $A_{2,2}$, $B_{2,2}$, $A_{2,3}$, and $B_{2,3}$ as (21). If we substitute (21) into (56), we can obtain the explicit expression for the optimal relay deployment $g_{3\mathrm{TS,opt}}$ in (17). Similarly, if we substitute (56) into (55), we can get the explicit expression for $\eta^{\mathrm{opt}}_{\mathrm{ECI,3TS}}$ in (19), which is the ECI of the 3TS transmission at the optimal relay deployment. ■

Appendix C
Proof of Theorem 3

In the 2TS scheme, the RN receives the signal from the BS and the UE simultaneously, and the received signals cannot be decoded with the traditional DF protocol. Thus, Nam *et al.* [7] proposed the use of nested lattice codes and structured binning to encode and decode the signals. The achievable rate of the proposed scheme in [7] is within 1/2 bit from the capacity region for each user. The expressions for the achievable rates are

$$R_{\mathrm{BS}\to\mathrm{UE,2TS}} = \mathbf{min}\left\{ \left[\frac{1}{2}B\log_2(\varsigma_1 + \varsigma_3)\right]^+ \frac{1}{2}B\log_2\left(1 + \frac{|h_{\mathrm{RN}\to\mathrm{UE}}|^2 P_{\mathrm{out.RN}}}{\sigma^2}\right)\right\} \tag{58}$$

$$R_{\mathrm{UE}\to\mathrm{BS,2TS}} = \mathbf{min}\left\{ \left[\frac{1}{2}B\log_2(\varsigma_2 + \varsigma_4)\right]^+ \frac{1}{2}B\log_2\left(1 + \frac{|h_{\mathrm{RN}\to\mathrm{BS}}|^2 P_{\mathrm{out.RN}}}{\sigma^2}\right)\right\} \tag{59}$$

where $[x]^+ \triangleq \mathbf{max}\{x, 0\}$, and

$$\begin{aligned} \varsigma_1 &= \frac{|h_{\mathrm{BS}\to\mathrm{RN}}|^2 P_{\mathrm{out,BS}}}{|h_{\mathrm{BS}\to\mathrm{RN}}|^2 P_{\mathrm{out,BS}} + |h_{\mathrm{UE}\to\mathrm{RN}}|^2 P_{\mathrm{out,UE}}} \\ \varsigma_2 &= \frac{|h_{\mathrm{UE}\to\mathrm{RN}}|^2 P_{\mathrm{out,UE}}}{|h_{\mathrm{BS}\to\mathrm{RN}}|^2 P_{\mathrm{out,BS}} + |h_{\mathrm{UE}\to\mathrm{RN}}|^2 P_{\mathrm{out,UE}}} \\ \varsigma_3 &= \frac{|h_{\mathrm{BS}\to\mathrm{RN}}|^2 P_{\mathrm{out,BS}}}{\sigma^2} \\ \varsigma_4 &= \frac{|h_{\mathrm{UE}\to\mathrm{RN}}|^2 P_{\mathrm{out,UE}}}{\sigma^2}. \end{aligned} \tag{60}$$

The sum of the total power consumption in the 2TS scheme is

$$P_{s,\mathrm{2TS}} = \frac{1}{2}\left(\rho_{\mathrm{BS}}\gamma_{\mathrm{BS}}\sqrt{P_{\mathrm{out,BS}}} + \rho_{\mathrm{UE}}\overline{m_{\mathrm{idle}}}\sqrt{P_{\mathrm{out,UE}}} + \rho_{\mathrm{RN}}\gamma_{\mathrm{RN}}\sqrt{P_{\mathrm{out,RN}}}\right) + C_{\mathrm{2TS}} \tag{61}$$

where $C_{\mathrm{2TS}} = (P_{C,\mathrm{BS}} + P_{C,\mathrm{UE}} + P_{C,\mathrm{RN}})/2$ is the sum of the constant power consumed by other parts beside the RF part in the BS, the relay, and the UE in the 2TS transmission scheme. Then, the optimization problem in (11) for the 2TS scheme turns into

$$\begin{aligned} \min_{g} \quad & \eta_{\mathrm{ECI,2TS}} = \frac{P_{s,\mathrm{2TS}}}{R_s} \\ \text{s.t.} \quad & R_{\mathrm{BS}\to\mathrm{UE,2TS}} = \beta R_s \\ & R_{\mathrm{UE}\to\mathrm{BS,2TS}} = (1-\beta)R_s. \end{aligned} \tag{62}$$

From the constraints, we can derive the expressions for $P_{\mathrm{out,BS}}$, $P_{\mathrm{out,UE}}$, and $P_{\mathrm{out,RN}}$ as follows:

$$\begin{aligned} P_{\mathrm{out,BS}} &= A^2_{3,1}\left(\frac{1}{1+g}\right)^{\alpha}, \quad P_{\mathrm{out,UE}} = B^2_{3,1}\left(\frac{g}{1+g}\right)^{\alpha} \\ P_{\mathrm{out,RN}} &= \mathbf{max}\left\{A^2_{3,2}\left(\frac{g}{1+g}\right)^{\alpha}, \quad B^2_{3,2}\left(\frac{1}{1+g}\right)^{\alpha}\right\} \end{aligned} \tag{63}$$

where the expressions for $A^2_{3,1}$, $B^2_{3,1}$, $A^2_{3,2}$, and $B^2_{3,2}$ are

$$A^2_{3,1} = \frac{\sigma^2}{\tau_0 d_0^{\alpha}}\frac{\mu_5}{\mu_5 + \mu_6}(\mu_5 + \mu_6 - 1)D^{\alpha}$$

$$B_{3,1}^2 = \frac{\sigma^2}{\tau_0 d_0^\alpha}\frac{\mu_6}{\mu_5+\mu_6}(\mu_5+\mu_6-1)D^\alpha$$
$$A_{3,2}^2 = \frac{\sigma^2}{\tau_0 d_0^\alpha}D^\alpha(\mu_5-1)$$
$$B_{3,2}^2 = \frac{\sigma^2}{\tau_0 d_0^\alpha}D^\alpha(\mu_6-1) \quad (64)$$

with $\mu_5 = 2^{2\beta R_s/B}$ and $\mu_6 = 2^{2(1-\beta)R_s/B}$.

Substitute (63) into the optimization objective function in (62), we have

$$\eta_{\mathrm{ECI,2TS}}(g) = f_{2\mathrm{TS}}(g) = \mathbf{max}\left\{f_{2\mathrm{TS},1}(g), f_{2\mathrm{TS},1}(g)\right\} \quad (65)$$

where the expressions for $f_{2\mathrm{TS},1}(g)$ and $f_{2\mathrm{TS},2}(g)$ are

$$f_{2\mathrm{TS},1}(g) = A_{3,3}\left(\frac{1}{1+g}\right)^{\frac{\alpha}{2}} + B_{3,3}\left(\frac{g}{1+g}\right)^{\frac{\alpha}{2}} + \frac{C_{2\mathrm{TS}}}{R_s} \quad (66)$$

$$f_{2\mathrm{TS},2}(g) = A_{3,4}\left(\frac{1}{1+g}\right)^{\frac{\alpha}{2}} + B_{3,4}\left(\frac{g}{1+g}\right)^{\frac{\alpha}{2}} + \frac{C_{2\mathrm{TS}}}{R_s} \quad (67)$$

where the expressions for $A_{3,3}$, $B_{3,3}$, $A_{3,4}$, and $A_{3,4}$ are

$$A_{3,3} = \frac{1}{2R_s}\rho_{\mathrm{BS}}\gamma_{\mathrm{BS}}A_{3,1}$$
$$B_{3,3} = \frac{1}{2R_s}(\rho_{\mathrm{UE}}\overline{m_{\mathrm{idle}}}B_{3,1} + \rho_{\mathrm{RN}}\gamma_{\mathrm{RN}}A_{3,2})$$
$$A_{3,4} = \frac{1}{2R_s}(\rho_{\mathrm{BS}}\gamma_{\mathrm{BS}}A_{3,1} + \rho_{\mathrm{RN}}\gamma_{\mathrm{RN}}B_{3,2})$$
$$B_{3,4} = \frac{1}{2R_s}\rho_{\mathrm{UE}}\overline{m_{\mathrm{idle}}}B_{3,1}. \quad (68)$$

Let $f_{2\mathrm{TS,dif}}(g)$ denote the difference between $f_{2\mathrm{TS},1}(g)$ and $f_{2\mathrm{TS},2}(g)$, i.e.,

$$\begin{aligned} f_{3\mathrm{TS,dif}}(g) &= f_{2\mathrm{TS},1}(g) - f_{2\mathrm{TS},2}(g) \\ &= (A_{3,3}-A_{3,4})\left(\frac{1}{1+g}\right)^{\frac{\alpha}{2}} \\ &\quad + (B_{3,3}-B_{3,4})\left(\frac{g}{1+g}\right)^{\frac{\alpha}{2}}. \end{aligned} \quad (69)$$

Then, the threshold for $f_{2\mathrm{TS}}(g)$ is the solution to $f_{2\mathrm{TS,dif}}(g) = 0$, i.e.,

$$g_{2\mathrm{TS,th}} = \left(\frac{A_{3,4}-A_{3,3}}{B_{3,3}-B_{3,4}}\right)^{\frac{2}{\alpha}}. \quad (70)$$

To decide when $f_{2\mathrm{TS}}(g) = f_{2\mathrm{TS},1}(g)$ and when $f_{2\mathrm{TS}}(g) = f_{2\mathrm{TS},2}(g)$, the derivative of $f_{2\mathrm{TS,dif}}(g)$ with respect to g is calculated as follows:

$$\begin{aligned} \frac{\partial f_{2\mathrm{TS,dif}}}{\partial g} &= (A_{3,4}-A_{3,3})\left(\frac{1}{1+g}\right)^{\frac{\alpha}{2}+1} \\ &\quad + (B_{3,3}-B_{3,4})\left(\frac{1}{1+g}\right)^{\frac{\alpha}{2}+1} g^{\frac{\alpha}{2}-1}. \end{aligned} \quad (71)$$

From (71), we can conclude that $\partial f_{2\mathrm{TS,dif}}/\partial g > 0$ for all $g > 0$, that is to say, $f_{2\mathrm{TS,dif}}(g)$ is an increasing function. Thus, we have the explicit expression for $f_{2\mathrm{TS}}(g)$ as

$$f_{2\mathrm{TS}}(g) = \begin{cases} f_{2\mathrm{TS},2}(g), & \text{if } g < g_{2\mathrm{TS,th}} \\ f_{2\mathrm{TS},1}(g), & \text{if } g \geq g_{2\mathrm{TS,th}}. \end{cases} \quad (72)$$

Based on (72), we can conclude that the optimal relay deployment will be achieved at the extreme points of $f_{2\mathrm{TS},2}$ and $f_{2\mathrm{TS},1}$ or the threshold $g_{2\mathrm{TS,th}}$. Thus, we have

$$g_{2\mathrm{TS,opt}} = \begin{cases} g_4 = \left(\frac{A_{3,4}}{B_{3,4}}\right)^{\frac{2}{\alpha-2}}, & \text{if } g_4 < g_{2\mathrm{TS,th}} \\ g_3 = \left(\frac{A_{3,3}}{B_{3,3}}\right)^{\frac{2}{\alpha-2}}, & \text{if } g_3 \geq g_{2\mathrm{TS,th}} \\ g_{2\mathrm{TS,th}} = \left(\frac{A_{3,4}-A_{3,3}}{B_{3,3}-B_{3,4}}\right)^{\frac{2}{\alpha}}, & \text{otherwise.} \end{cases} \quad (73)$$

Therefore, the optimal relay deployment for the 2TS scheme is

$$d_{\mathrm{RN}\to\mathrm{UE}}^{2\mathrm{TS}} = g_{2\mathrm{TS,opt}} d_{\mathrm{BS}\to\mathrm{RN}}^{2\mathrm{TS}}. \quad (74)$$

If we substitute (64) into (68), we can get the explicit expressions for $A_{3,3}$, $B_{3,3}$, $A_{3,4}$, and $B_{3,4}$ in (28). If we substitute (28) into (73), we can get the explicit expression for $g_{2\mathrm{TS,opt}}$ in (23). If we substitute (73) into (72), we can obtain the explicit expression for $\eta_{\mathrm{ECI,2TS}}^{\mathrm{opt}}$ in (26). ■

REFERENCES

[1] J. Sydir and R. Taori, "An evolved cellular system architecture incorporating relay stations," *IEEE Commun. Mag.*, vol. 47, no. 6, pp. 115–121, Jun. 2009.

[2] Z. Hasan, H. Boostanimehr, and V. K. Bhargava, "Green cellular networks: A survey, some research issues and challenges," *IEEE Commun. Surveys Tuts.*, vol. 13, no. 4, pp. 524–540, 4th Qtr.

[3] S. McLaughlin, P. M. Grant, J. S. Thompson, H. Haas, D. I. Laurenson, C. Khirallah, Y. Hou, and R. Wang, "Techniques for improving cellular radio base station energy efficiency," *IEEE Wireless Commun.*, vol. 18, no. 5, pp. 10–17, Oct. 2011.

[4] R. Ahlswede, N. Cai, S.-Y. R. Li, and R. W. Yeung, "Network information flow," *IEEE Trans. Inf. Theory*, vol. 46, no. 4, pp. 1204–1216, Jul. 2000.

[5] S. Zhang, S.-C. Liew, and P. P. Lam, "Hot topic: Physical-layer network coding," in *Proc. 12th Annu. Int. Conf. MOBICOM Netw.*, Sep. 2006, pp. 358–365.

[6] S. Katti, H. Rahul, W. Hu, D. Katabi, M. Medard, and J. Crowcroft, "XORs in the air: Practical wireless network coding," *IEEE/ACM Trans. Netw.*, vol. 16, no. 3, pp. 497–510, Jun. 2008.

[7] W. Nam, S. Y. Chung, and Y. H. Lee, "Capacity of the Gaussian two-way relay channel to within 1/2 bit," *IEEE Trans. Inf. Theory*, vol. 56, no. 11, pp. 5488–5494, Nov. 2010.

[8] W. Zhang, D. Duan, and L. Yang, "Relay selection from a battery energy efficiency perspective," *IEEE Trans. Commun.*, vol. 59, no. 6, pp. 1525–1529, Jun. 2011.

[9] X. He and F. Y. Li, "Throughput and energy efficiency comparison of one-hop, two-hop, virtual relay and cooperative retransmission schemes," in *Proc. EW Conf.*, Apr. 2010, pp. 580–587.

[10] Y. Yao, X. Cai, and G. B. Giannakis, "On energy efficiency and optimum resource allocation of relay transmissions in the low-power regime," *IEEE Trans. Wireless Commun.*, vol. 4, no. 6, pp. 2917–2927, Nov. 2005.

[11] C. Sun and C. Yang, "Energy efficiency analysis of one-way and two-way relay systems," *EURASIP J. Wireless Commun. Netw.*, vol. 2012, no. 1, pp. 1–18, Feb. 2012.

[12] J. Zhang, L. L. Yang, and L. Hanzo, "Energy-efficient dynamic resource allocation for opportunistic-relaying-assisted SC-FDMA using turbo-equalizer-aided soft decode-and-forward," *IEEE Trans. Veh. Technol.*, vol. 62, no. 1, pp. 235–246, Jan. 2013.

[13] N. Abuzainab and A. Ephremides, "Energy efficiency of cooperative relaying over a wireless link," *IEEE Trans. Wireless Commun.*, vol. 11, no. 6, pp. 2076–2083, Jun. 2012.

[14] A. Zafar, R. M. Radaydeh, Y. Chen, and M.-S. Alouini, "Energy-efficient power allocation for fixed-gain amplify-and-forward relay networks with partial channel state information," *IEEE Wireless Commun. Lett.*, vol. 1, no. 6, pp. 553–556, Dec. 2012.
[15] F. Parzysz, M. Vu, and F. Gagnon, "Energy minimization for the half-duplex relay channel with decode-forward relaying," *IEEE Trans. Commun.*, vol. 61, no. 6, pp. 2232–2247, Jun. 2013.
[16] Y. Li, X. Zhang, M. Peng, and W. Wang, "Power provisioning and relay positioning for two-way relay channel with analog network coding," *IEEE Signal Process. Lett.*, vol. 18, no. 9, pp. 517–520, Sep. 2011.
[17] C. Khirallah, J. S. Thompson, and H. Rashvand, "Energy and cost impacts of relay and femtocell deployments in long-term-evolution advanced," *IET Commun.*, vol. 5, no. 18, pp. 2617–2628, Dec. 2011.
[18] G. Wu and G. Feng, "Energy-efficient relay deployment in next generation cellular networks," in *Proc. IEEE ICC*, 2012, pp. 5757–5761.
[19] B. Lin and L. Lin, "Site planning of relay stations in green wireless access networks: A genetic algorithm approach," in *Proc. Int. Conf. SoCPaR*, 2011, pp. 167–172.
[20] M. Zhou, Q. Cui, J. Riku, and X. Tao, "Energy-efficient relay selection and power allocation for two-way relay channel with analog network coding," *IEEE Commun. Lett.*, vol. 16, no. 6, pp. 816–819, Jun. 2012.
[21] C. Y. Ho and C. Y. Huang, "Energy efficient subcarrier-power allocation and relay selection scheme for OFDMA-based cooperative relay networks," in *Proc. IEEE ICC*, 2011, pp. 1–6.
[22] H. Karl, "An overview of energy-efficiency techniques for mobile communication systems," Univ. Berlin, Berlin, Germany, TKN Tech. Rep., 2003.
[23] G. Kramer, M. Gastpar, and P. Gupta, "Cooperative strategies and capacity theorems for relay networks," *IEEE Trans. Inf. Theory*, vol. 51, no. 9, pp. 3037–3063, Sep. 2005.
[24] A. Goldsmith, *Wireless Communications*. Cambridge, U.K.: Cambridge Univ. Press, 2005.
[25] A. Gunther, B. Oliver, G. Vito, G. Istvan, A. I. Muhammad, J. Ylva, K. Efstathios, O. Magnus, S. Dario, S. Per, and W. Wieslawa, "Energy efficiency analysis of the reference systems, areas of improvements and target breakdown," INFSO-ICT-247733 EARTH Deliverable D2.3 2010.
[26] A. B. Saleh, S. Redana, B. Raaf, and J. Hamalainen, "Comparison of relay and pico eNB deployments in LTE-advanced," in *Proc. IEEE VTC Fall*, 2009, pp. 1–5.
[27] A. R. Jensen, M. Lauridsen, P. Mogensen, T. B. Sorensen, and P. Jensen, "LTE UE power consumption model: For system level energy and performance optimization," in *Proc. IEEE VTC Fall*, 2012, pp. 1–5.
[28] G. Lim and L. J. Cimini, "Energy-efficient cooperative relaying in heterogeneous radio access networks," *IEEE Wireless Commun. Lett.*, vol. 1, no. 5, pp. 476–479, Oct. 2012.
[29] "High efficiency power amplifier," presented at the 3rd Generation Partnership Project (3GPP) TSG-RAN WG4 Meeting #66bis, Apr. 15–19, 2013, Paper R4-131752.
[30] M. M. A. Hossain and R. Jantti, "Impact of efficient power amplifiers in wireless access," in *Proc. IEEE Online Conf. GreenCom*, 2011, pp. 36–40.
[31] "Base Station (BS) radio transmission and reception," 3GPP TS 36.104, 2007.
[32] "Further advancements for E-UTRA physical layer aspects," 3rd Generation Partnership Project (3GPP), Sophia-Antipolis, France, 3GPP TR 36.814, 2010.

Qimei Cui (M'11) received the B.E. and M.S. degrees in electronic engineering from Hunan University, Changsha, China, in 2000 and 2003, respectively, and the Ph.D. degree in telecommunications from the Beijing University of Posts and Telecommunications (BUPT), Beijing, China, in 2006.

She is currently an Associate Professor with the BUPT. She has published over 50 technical papers and filed seven patents. Moreover, seven of her submitted proposals have been accepted by the 3GPP LTE-A standardization group by collaborating with corporations. Her research interests mainly focus on transmission theories, networking technologies, green communications, and 3GPP LTE-A standardization for next-generation mobile communication networks.

Dr. Cui received the only Best Paper Award at the 12th IEEE International Symposium on Communications and Information Technologies (ISCIT 2012) and the Honoured Mentioned Demo Award at the 15th ACM International Conference on Mobile Computing and Networking (MobiCom 2009).

Xianjun Yang received the B.E. degree in communication engineering from Yantai University, Yantai, China, in 2008. She is currently working toward the joint M.S./Ph.D. degree in telecommunications with the Beijing University of Posts and Telecommunications (BUPT), Beijing, China, and the joint Ph.D. degree (Cotutelle program) with Macquarie University, Sydney, Australia.

From September 2011 to March 2012, she was a Visiting Ph.D. Student with the Information and Communication Technologies Center, Commonwealth Scientific and Industrial Research Organization, Australia, sponsored by the China Scholarship Council. Her research interests include green communications, compressed sensing (CS), and the application of CS in wireless sensor networks and cognitive radio networks.

Jyri Hämäläinen (M'09) received the M.Sc. and Ph.D. degrees from the University of Oulu, Oulu, Finland, in 1992 and 1998, respectively.

From 1999 to 2007, he was with Nokia, where he worked on various aspects of mobile communication systems. Since 2008, he has been a Professor with the Department of Communications and Networking, Aalto University School of Electrical Engineering, Aalto, Finland. He is the author or coauthor of more than 140 scientific publications. He is the holder of 35 U.S. patents or patent applications. His research interests include multiantenna transmission and reception techniques, radio resource scheduling, relays, small cells, and the design and analysis of wireless networks in general.

Xiaofeng Tao (SM'13) received the B.S. degree in electrical engineering from Xi'an Jiaotong University, Xi'an, China, in 1993 and the M.S.E.E. and Ph.D. degrees in telecommunication engineering from the Beijing University of Posts and Telecommunications (BUPT), Beijing, China, in 1999 and 2002, respectively.

He was a Visiting Professor with Stanford University, Stanford, CA, USA, from 2010 to 2011; the Chief Architect of the Chinese National FuTURE Fourth-Generation (4G) TDD working group from 2003 to 2006; and established the 4G TDD CoMP trial network in 2006. He is currently a Professor with the BUPT and a Fellow of the Institution of Engineering and Technology. He is the inventor or coinventor of 50 patents and the author or coauthor of 120 papers in 4G and beyond 4G.

Ping Zhang (M'11) received the Ph.D. degree from the Beijing University of Posts and Telecommunications (BUPT), Beijing, China, in 1990.

He is currently a Professor with the BUPT, the Director of the Wireless Technology Innovation Labs, and the Vice Director of the Ubiquitous Networking Task Commission of the China Communications Standards Association. He is the Chief Scientist of the National Program on Key Basic Research Project (973 Program). He also serves as a member of the China 3G Group, China 863 FuTURE project. As Project Leader or Principal Investigator, he has taken on many important national and enterprise projects. He is the author or coauthor of more than 200 journal/conference papers. He has more than 100 patent applications, 35 of which have been authorized. His research interests mainly focus on the fields of mobile communications, ubiquitous networking, and service provisioning.

Dr. Zhang has served as the Technical Program Committee Member of a series of international conferences, such as the International Symposium on Personal, Indoor, and Mobile Radio Communications and the Vehicular Technology Conference, among others. For his many achievements, he has received many honors and awards from the Chinese government and the Educational Ministry. He is also one of the few professors that enjoy the Government Special Allowance in China.